Perspective

Integrated Materials Design and Process Engineering for n-Type Polymer Thermoelectrics

Published as part of JACS Au special issue "Polymers for the Clean Energy Transition".

Xin-Yu Deng, Zhi Zhang, and Ting Lei*

Cite This: *JACS Au* 2024, 4, 4066−4083

Read Online

ACCESS | Metrics & More | Article Recommendations

ABSTRACT: Polymer thermoelectrics (TEs) have attracted increasing interest in recent years, owing to their great potential in intimate integration with wearable electronics for powering small electronics/sensors and personal temperature regulation. Over the past few decades, substantial progress has been made in enhancing polymer TE performance. However, the electrical conductivity and power factor of most n-doped polymers are about an order of magnitude lower than those of their p-type counterparts, impeding the development of highly efficient polymer TE devices. In addition, unlike well-studied inorganic materials, the complex charge transport mechanism and polymer−dopant interactions in polymer TE materials have hindered a comprehensive under-standing of the structure−property relationships. This Perspective aims to survey recent achievements in understanding the charge transport mechanism and selectively provide some critical insights into molecular design and process engineering for n-type polymer TEs. We also highlight the great potential of polymer TEs in wearable electronics and offer an outlook for future development.

KEYWORDS: *conjugated polymers, organic thermoelectrics, charge transport, molecular design, flexible stretchable device*
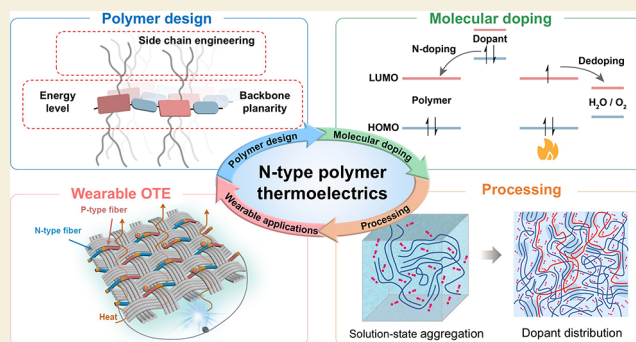
1. INTRODUCTION

Thermoelectrics (TEs) are gaining significant importance due to their unique ability to directly convert heat into electricity and vice versa through Seebeck and Peltier effects, respectively. They can convert waste heat from industrial processes, automobiles, and even human bodies to useful electrical energy. Recently, flexible TEs are becoming more important since they can be integrated with wearable electronics to power small electronic devices and sensors by harvesting body heat. Among various TE materials, polymer TE materials have attracted increasing interest, because of their low toxicity, lightweight, good solution processability, high mechanical flexibility, and good perform-ance at room temperature range.[1−3]

The energy-conversion efficiency of a thermoelectric material is evaluated by the figure-of-merit (*ZT*):

$$ZT = \frac{S^2\sigma}{\kappa}T \tag{1}$$

Where *T* is the absolute temperature, and *S*, *σ*, and *κ* are the Seebeck coefficient, electrical conductivity, and thermal conductivity, respectively. Although both state-of-the-art p- and n-type polymers have achieved *ZT* values over 0.3,[4,5] these performances still lag behind that of the inorganic counterparts.

In addition, *ZT* values over 1.0 with good stability are expected for commercial applications. Further enhancement of the thermoelectric performance of conjugated polymers is highly desirable. Since conjugated polymers usually have low thermal conductivities, the main method to achieve high TE perform-ance is to improve the power factor (*PF*):

$$PF = S^2\sigma \tag{2}$$

In which *σ* and *S* can be described as

$$\sigma = en\mu \tag{3}$$

$$S = \frac{k_B}{e} \int \frac{E - E_F}{k_B T} \frac{\sigma(E)}{\sigma} dE \tag{4}$$

Where *e* is the elementary charge, *n* is the charge carrier concentration, *μ* is the carrier mobility, k_B is the Boltzmann
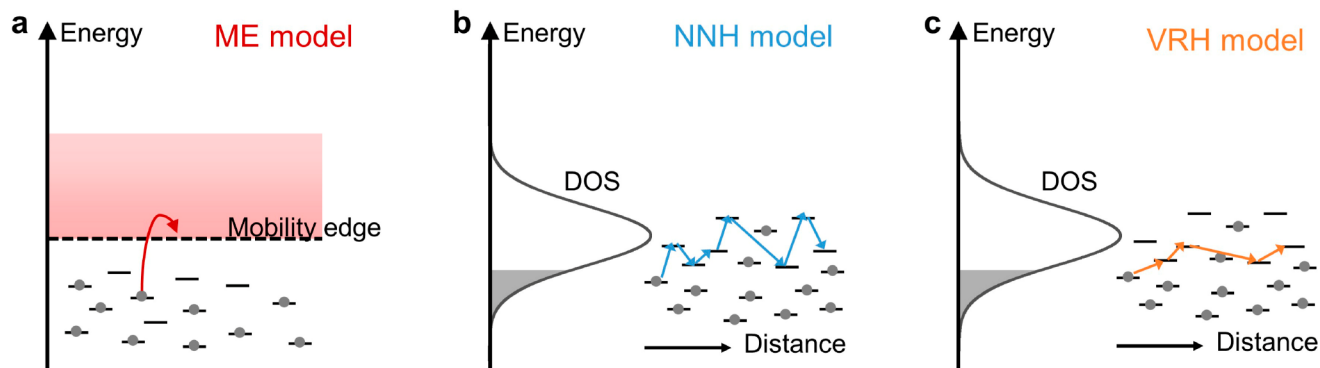
Figure 1. Schematic illustrating charge transport in (a) Mott's mobility edge model, (b) Nearest neighbor hopping model, and (c) Variable range hopping model.

constant, and E_F is the Fermi level. Pristine polymer semiconductors cannot directly function as TE materials, owing to their low n and σ. Thus, molecular doping is indispensable for polymer TEs to increase n.[6,7] While a high n can contribute to an increase in σ, it also inevitably results in a decrease in S. These interrelated parameters make improving the ZT values particularly complicated.

To achieve a high-performance thermoelectric device, it is essential to have both p- and n-type conjugated polymers with comparable performance. To date, p-type conjugated polymers have demonstrated excellent conductivities exceeding 1000 S cm^{-1}, along with high power factors over 300 μW m^{-1} K^{-2}.[5,8] In contrast, only a few n-type conjugated polymers have shown conductivities over 100 S cm^{-1} and power factors over 100 μW m^{-1} K^{-2}.[9−11] To optimize the TE performance of n-type conjugated polymers, researchers have developed various molecular design guidelines and doping strategies.[7,12,13] A notable development is the side-chain-free n-type polymer PBFDO (or n-PBDF), which exhibited a high conductivity over 2000 S cm^{-1}.[14,15] Nevertheless, the Seebeck coefficient (-21 μV K^{-1}) and power factor (90 μW m^{-1} K^{-2}) of this metallic polymer are modest, indicating significant room for improvement. Despite this specific advancement, a systematic improvement in the TE performance of the n-type polymer still remains absent. The field urgently requires clear guidelines to identify and prioritize research directions for further development.

In this Perspective, we begin with a brief introduction to charge transport theories in doped conjugated polymers. While there is no universal model applicable to all kinds of doped conjugated polymers, we identify the critical roles of energetic disorder and charge carrier density in determining thermoelectric performance. Based on these theoretical understandings, we highlight some critical molecular designs and effective processing strategies that have led to substantial progress for n-type polymer TEs. We also discuss the dependence of thermal conductivities on the molecular structure, areas that have received limited attention. Additionally, we present the potential of polymer thermoelectrics for wearable and flexible electronics. Finally, we discuss the current challenges and opportunities for polymer TE materials.

2. CHARGE TRANSPORT THEORY

Thermoelectric properties of conjugated polymers are based on their charge transport properties. Understanding their charge transport mechanism is the theoretical basis for the development of high-performance materials. However, unlike inorganic

crystals, the conjugated polymer film is heterogeneous, including crystalline and amorphous regions. The disordered nature, abundant structural defects, and localized carriers of conjugated polymers result in a complicated charge transport mechanism. In addition, the OTE needs materials to operate effectively in heavily doped states, where the charge transport could be different from the pristine states. Up to now, there is no universal charge transport model that can apply to all kinds of conjugated polymers. Here, we give a brief summary of the widely used charge transport model, trying to build a relationship between the charge transport mechanism and thermoelectric performance.

Considering the localized carrier in conjugated polymers, the charge transport can be simply described by Mott's mobility edge (ME) model. Charge carriers with energy above the mobility edge freely conduct electricity like a metal, while localized carriers with energy lower than the mobility edge need to be thermally activated to contribute to conductivity (Figure 1a).[16] Mott assumes the nondegenerate limit where $\frac{E_c - E_F}{k_B T} \ll -1$, and describes σ:

$$\sigma = \sigma_0 \exp\left(-\frac{E_C - E_F}{k_B T}\right) \tag{5}$$

Where σ_0, E_C, E_F, k_B, and T are the conductivity at the mobility edge in the 0 K limit, mobility edge, Fermi energy, Boltzmann's constant, and temperature, respectively. The ME model is successful in describing the charge transport in polycrystalline polymers, such as PQT-12[17] and P3HT.[18] However, the experimental conductivity of most doped conjugated polymers is always thermally activated, leading to the failure of this model.

Unlike the ME model, hopping models assume that charge transport in disordered conjugated polymers occurs via hopping between localized sites. The nearest neighbor hopping model (NNH) describes that carriers would preferentially hop to the spatially nearest sites (Figure 1b).[19] When the energy difference of nearest neighbor sites is too large, the carrier tends to hop to a site with close energy but a larger distance, called variable range hopping (VRH) transport model (Figure 1c).[20] The charge transport behavior of VRH can be expressed as

$$\sigma_{VRH} = \sigma_0 \exp\left[-\left(\frac{T_0}{T}\right)^r\right] \tag{6}$$

Where σ_0, T_0, and γ are the pre-exponential factor, characteristic temperature, and hopping index, respectively.[21] Unlike the constant hopping distance in NNH, in VRH, any change in

temperature or DOS shape leads to a change in both the hopping distance and the energy difference between sites, consequently changing the charge transport path. Compared with the polymers described by the NNH model, the polymers described by the VRH model often have higher conductivity and smaller Seebeck coefficients at the same carrier concentration.[22,23] The Seebeck coefficients produced from the VRH model are generally on the order of 10 μV K^{-1}, which is much lower than the experimental results. The failure of both the mobility edge and hopping models indicates the difficulty of using a single model to describe the thermoelectric properties of doped conjugated polymers. It may be a challenge to clearly define the delocalized or localized charge carrier concentration and mobility in such complex systems.

To solve this issue, Kang and Snyder avoid this complication and analyze the conductivity in a much more generalized form.[24] In the Kang−Snyder model, electrical conductivity σ can be expressed as

$$\sigma = \int \sigma_E \left(-\frac{\partial f}{\partial E} \right) dE \tag{7}$$

$$\sigma_E(E, T) = \begin{cases} \sigma_{E_0}(T) \times \left(\dfrac{E - E_t}{k_B T} \right)^s, & (E > E_t) \\ \\ 0, & (E < E_t) \end{cases} \tag{8}$$

And the Seebeck coefficient becomes

$$S = \frac{1}{\sigma} \frac{k_B}{e} \int \frac{E - E_F}{k_B T} \sigma_E \left(-\frac{\partial f}{\partial E} \right) dE \tag{9}$$

Where f is the Fermi−Dirac distribution function, $\frac{E}{k_B T}$ is the reduced energy of the charge carriers, and $\sigma_{E_0}(T)$ is the transport coefficient. By combining eq 8 and 9, the Seebeck-conductivity relation can be obtained: $S \propto \sigma^{-1/s}$. When $s = 0$, it turns into the ME model. When $s > 0$, conductivity is thermally activated even for carriers with energy above the transport edge. For typical conducting polymers, such as PBTTT and P3HT, the S−σ curve is well described by $s = 3$. In contrast, high-performance PEDOT-based samples fit better with $s = 1$. However, the physical relationships governing s of the Kang−Snyder model are not clear.

Recently, Hippalgaonkar, Wu, and co-workers attributed the difference of s in the Kang−Snyder model to different scattering mechanisms and the broadening of the density of states (DOS).[25] In their model, they used a new exponential parameter, r. They found that doped conjugated polymers that have stronger energy-dependent scattering, $r = 1.5$, exhibit higher power factors than those with $r = -0.5$, which is similar to $s = 1$ and $s = 3$ in the Kang−Snyder model. For example, PEDOT-based polymers, which have more backbone vibrations due to the lack of side chains, are best modeled when $r = -0.5$. In contrast, P3HT and PBTTT exhibit $r = 1.5$, suggesting that the dominant scattering mechanism is determined by the ionized counterions. They also demonstrated that the width of Gaussian DOS (w) increases exponentially with paracrystallinity. For PBTTT and P3HT, w values are smaller (0.1−0.3 eV) than those found for PEDOT:PSS ($w \sim 0.8$ eV). This is consistent with the fact that polymers with side chains tend to show higher crystallinity with narrower DOS tails. Compared with the Kang−Snyder mode, this study provides deeper physical

insights into the distinct charge transport mechanisms in conducting polymers.

However, several studies have demonstrated inconsistency between experimental data and the Kang−Snyder model.[26−28] One of the main concerns is the neglect of carrier concentration dependence in charge transport. As the carrier density increases, the distance R between localization traps decreases, which eventually leads to the overlap of the wells and lowers the depth of potential wells W_H (Figure 2a).[29,30] Therefore, the transport
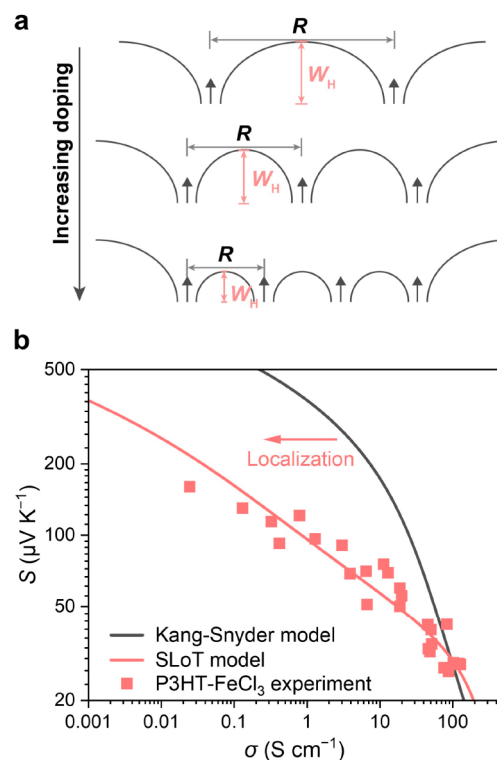
Figure 2. (a) Charge carriers are localized in potential energy wells W_H, which are separated from each other by a distance R that depends on the carrier density n and carrier concentration ratio c. (b) S−σ plot. Red squares represent the P3HT-FeCl$_3$ experimental data from ref 31. The red line fits these data using the SLoT model, and the black line corresponds to the Kang−Snyder model with $s = 1$.

function σ_{E_0} is probably a function of carrier concentration through W_H. However, in the Kang−Snyder model, σ_{E_0} and W_H are constants for a given material. To capture transition in transport behavior in semiconducting polymers as a function of carrier concentration ratio c, Yee, Hanus, and co-workers developed the semilocalized transport (SLoT) model:[31]

$$\sigma_E(E, T, c) = \begin{cases} \sigma_0 \exp\left(-\dfrac{W_H(c)}{k_B T} \right) \times \left(\dfrac{E - E_t}{k_B T} \right), & (E \geq E_t) \\ \\ 0, & (E < E_t) \end{cases} \tag{10}$$

A notable difference from the Kang−Snyder model is that the transport function's energy-independent term, $\sigma_{E_0}(T) = \sigma_0 \exp\left(-\frac{W_H(c)}{k_B T} \right)$, which is defined as a function of $W_H(c)$:
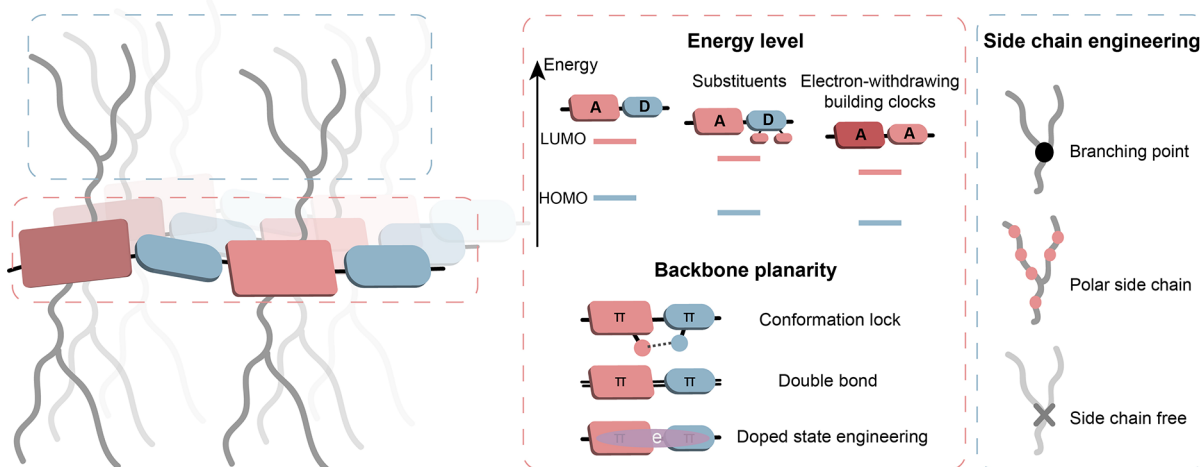
Figure 3. Schematic illustration of the molecular design in conjugated polymers toward achieving OTE applications.
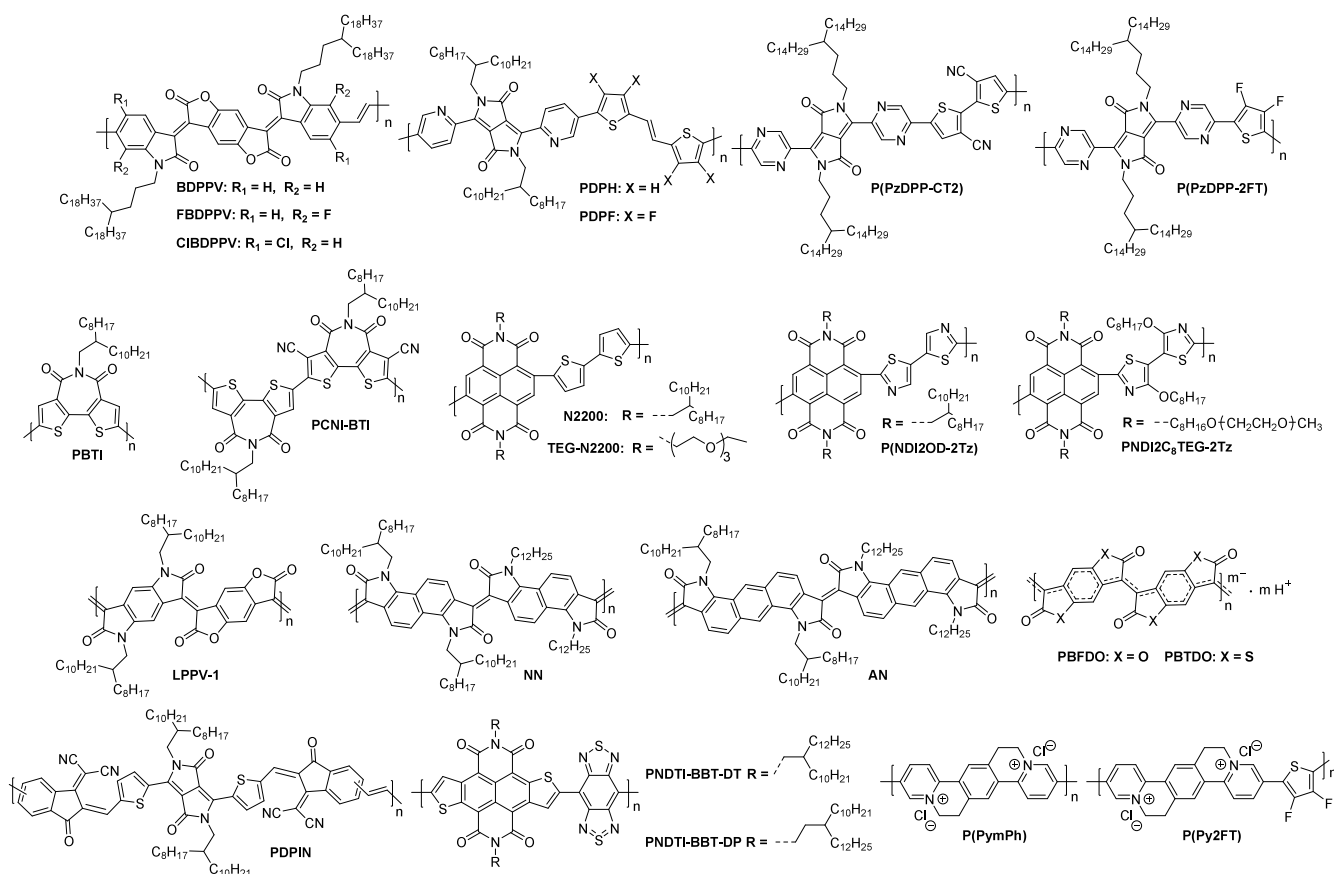

Figure 4. Chemical structures of n-type TE materials discussed in this perspective.

$$W_{\mathrm{H}}(c) = \begin{cases} W_{\mathrm{H}}^{\max} - W_{\mathrm{H}}^{slope} c^{1/3}, & (c \leq c_d) \\ 0, & (c > c_d) \end{cases} \quad (11)$$

Because both W_{H} and c are experimentally measurable, the maximum localization energy ($W_{\mathrm{H}}^{\max}$) and the rate at which localization decreases with increasing carrier ratio (W_{H}^{slope}) can be calculated. c_d is the carrier ratio where delocalized transport is achieved ($W_{\mathrm{H}} = 0$). The SLoT model exhibits delocalized transport consistent with the Kang−Snyder model at high doping concentrations but more accurately captures the transport phenomenon at low doping levels because of charge

carrier localization (Figure 2b). Although the SLoT model can fit experimental data from a wide range of chemical systems, including P3HT,[32] PBTTT,[27,33] PA,[34−38] PEDOT,[8] SWCNT,[39] and N2200,[26] it only describes the phenomenon of localized and delocalized transport and does not provide a direct correlation between the molecular structure and the charge transport properties.

To understand where there is room for improving the polymer TE performance, we try to identify the common key factors behind these different theoretical models. Interestingly, despite incorporating different parameters, the charge transport in these models is intimately associated with two factors:

energetic disorder and carrier density. For example, lower energetic disorders result in lower activation energies for carrier hopping and higher carrier mobilities. Increasing the carrier density usually decreases the carrier mobility but simultaneously reduces the trap depth and affects transport levels. Therefore, in this Perspective, we focus on recent important molecular design and doping considerations to reduce energetic disorder and increase carrier density.

3. POLYMER DESIGN

Typically, most polymer TEs consist of π-conjugated backbones and long side chains. Designing a conjugated backbone is powerful for tuning the energy levels and backbone planarity, which directly influence the carrier density and mobility. While side chains do not directly constitute the charge transport pathways, they could significantly affect the polymer solubility, packing order, and miscibility with dopants. Both the conjugated backbone and side chain design are essential for exploring high-performance polymer TEs. In this section, we discuss the molecular design strategies for both conjugated backbones and side chains, and divide them into three categories: energy level, backbone planarity, and side chain engineering (Figure 3). The chemical structures of conjugated polymers discussed in this Perspective are shown in Figure 4.

3.1. Energy Level

The energy level plays a crucial role in the optoelectronic properties of conjugated polymers. Tuning the energies and distributions of frontier molecular orbitals via chemical structure design is the most widely used strategy to control the performance of conjugated polymers. For n-doping, the dopant transfers electrons to the lowest unoccupied molecular orbital (LUMO) level of the polymers. To enhance the n-doping efficiency and reduce H_2O and O_2 trapping, a low-lying LUMO level is highly desired for n-type conjugated polymers.

Pei et al. developed a series of BDOPV-based conjugated polymers for n-type thermoelectric materials.[40] To reduce the LUMO levels of conjugated polymers, they incorporated fluorine and chlorine atoms into the BDPPV backbones, obtaining FBDPPV and ClBDPPV. The introduction of halogen substituents effectively lowered the LUMO levels from −4.01 eV (BDPPV) to −4.30 eV (FBDPPV) and −4.17 eV (ClBDPPV). After n-doping, both FBDPPV and ClBDPPV exhibited a higher doping efficiency and a dramatic enhancement in electrical conductivities. Notably, FBDPPV reached a high conductivity of 14 S cm^{-1}, yielding a power factor of 28 μW m^{-1} K^{-2}.

Besides substituents, introducing strong electron-withdrawing building blocks is also an effective way to lower the LUMO level. Our group designed and synthesized a new acceptor–acceptor (A-A) polymer P(PzDPP-CT2).[41] Among the most studied DPP building blocks, pyrazine-flanked DPP (PzDPP) showed the deepest LUMO energy level (Figure 5a). With an electron-deficient moiety, 3,3′-dicyano-2,2′-bithiophene, as the donor, P(PzDPP-CT2) exhibited a deep LUMO level down to −4.03 eV. After doping, this copolymer exhibited a high electrical conductivity of 8.4 S cm^{-1} and an n-type TE power factor of 57.3 μW m^{-1} K^{-2} (Figure 5b). Guo et al. also demonstrated that constructing A-A copolymers is effective in developing n-type conjugated polymers with a high thermoelectric performance. By introducing strong electron-withdrawing cyano functionality on BTI and its derivatives, they developed a series of novel electron-deficient building blocks.[42]
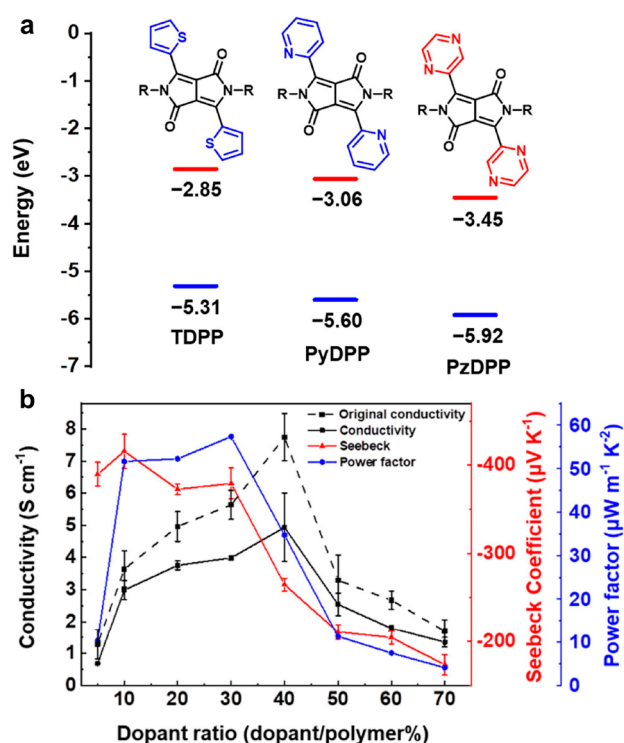

Figure 5. (a) Chemical structures and calculated HOMO/LUMO levels of the two most studied DPP building blocks (thiophene-flanked and pyridine-flanker DPP) and PzDPP. (b) Electrical conductivities, Seebeck coefficients, and power factors of P(PzDPP-CT2) at different dopant/polymer ratios. The dashed lines show the original conductivities measured in a nitrogen glovebox. The solid lines are the thermoelectric parameters measured under a vacuum chamber. Reproduced with permission from ref 41. Copyright 2019, American Chemical Society.

A-A type polymers based on these novel building blocks featured greatly suppressed LUMOs (−3.64 to −4.11 eV) compared to that of the reference polymer PBTI. Among them, PCNI-BTI reached the highest electrical conductivity of up to 23.3 S cm^{-1}, which is remarkably higher than that of PBTI (0.002 S cm^{-1}). This "lowering LUMO" strategy has not only effectively improved the doping efficiency but also enhanced the stability. Recently, the highly conductive n-type polymer PBFDO (also known as n-PBDF) has attracted considerable interest. It is synthesized by a combination of oxidative polymerization and in situ reductive n-doping.[14,15] As a result, the intrinsically doped PBFDO exhibits a LUMO of −5.1 eV, which is the lowest among all reported n-type conjugated polymers and is stable under air, moisture, and thermal conditions.

These results indicate that "lowering LUMO" plays an important role in optimizing the n-type polymer TE performance. However, a low LUMO level does not necessarily lead to high electrical conductivity. For example, Huang et al. reported another conducting polymer, PBTDO, which also has a deep LUMO.[43] Despite this, PBTDO only showed moderate electrical conductivity of 0.14 S cm^{-1}, in stark contrast to the highly conductive PBFDO. Density functional theory (DFT) calculations revealed that PBTDO exhibited distorted conjugated backbones, with dihedral angles greater than 25° between adjacent units, whereas PBFDO's dihedral angles are less than 6°. This distorted backbone conformation in PBTDO may limit carrier delocalization through the backbone, which in turn affects its doping levels. A recent theoretical study found

that only in the coplanar 2D networks of PBFDO, a metallic nature of the electronic structure is observed.[44] Interestingly, when stacking these 2D networks into various $\pi-\pi$ packing patterns, all of the resulting three-dimensional (3D) structures consistently exhibited a metallic nature. These findings suggest that, in addition to LUMO levels, factors such as backbone planarity and molecular packing should be considered.

3.2. Backbone Planarity

Since backbone planarity directly influences the intrachain charge delocalization and intermolecular π-orbital overlap, and consequently determines the charge transport,[45,46] considerable design strategies have been developed to improve the backbone coplanarity and rigidity. Conventional conjugated polymers typically use carbon–carbon single bonds to link building blocks. To lock the free rotation of these single bonds, intramolecular noncovalent interactions, such as S···O, S···F, and H···F, are used.[47−50] DFT calculations showed that the binding energies of these interactions can reach 2 kcal/mol (>3 kT),[51] providing effective conformation control under thermal fluctuations. Based on this concept, a new conjugated polymer, P(NDI2OD-2Tz), was synthesized by replacing the thiophene ring in P(NDI2OD-T2) with a thiazole ring.[52] The N···O interactions hinder the rotation of the dihedral angles, conducted to enhance backbone planarity and improve $\pi-\pi$ stacking. The power factor of P(NDI2OD-2Tz) reached 1.5 μW m^{-1} K^{-2}, which is 2 orders of magnitude enhancement compared to P(NDI2OD-T2). Pei and co-workers designed and synthesized a new DPP-based polymer, PDPF, by introducing fluorine atoms on the thiophene ring.[53] PDPF exhibits short H···F distances (2.25 Å/2.24 Å), and these distances are smaller than the sum of the van der Waals radii of F and H atoms (1.35 and 1.20 Å, respectively), indicating the formation of C−H···F bonds. With the "conformation lock" effect of H···F interactions, PDPF exhibited a coplanar conformation with negligible dihedral angles and a large energy barrier for molecular torsion. Compared to the reference polymer PDPH, the F-substituted PDPF exhibited a significantly higher electrical conductivity of 1.3 S cm^{-1} and a maximum power factor of 4.65 μW m^{-1} K^{-2}.

Another effective strategy is to change the single bonds into double bonds, leading to a rigid coplanar backbone conformation. Via aldol condensation reaction, poly(p-phenylenevinylene) (PPV) derivative LPPV-1 with completely fused backbone structures can be obtained, which do not contain any single-bond linkages.[54] LPPV-1 exhibited a maximum electrical conductivity of 1.1 S cm^{-1} and the power factor was up to 1.96 μW m^{-1} K^{-2}. Other double-bond conjugated polymers, such as NN and AN, were also reported with field-effect mobility up to 0.03 cm^2 V^{-1} s^{-1} and the electrical conductivity up to 0.65 S cm^{-1}.[55,56] Given the rigid rod-like backbone of these polymers, this level of achievable mobility and electrical conductivity is somewhat disappointing. Sirringhaus et al. found that the double-bond linkages in doped states largely stretch out compared to the neutral ground state, leading to a twisted backbone.[57] This twisted backbone acts against the polaron delocalization and slows the charge transport.

Currently, understanding the planarity in conjugated backbones mainly relies on DFT calculations to find the lowest energy conformation and rotation barriers. Since torsional potentials adopt various shapes, directly comparing the backbone planarity across different conjugated polymers is limited. To address this issue, Perepichka and Che proposed a new parameter, $\langle\cos^2\varphi\rangle$, based on a statistical analysis of conformational disorder to quantify the backbone planarity.[58] $\langle\cos^2\varphi\rangle$ is a better predictor of the molecular planarity than the commonly used lowest-energy dihedral angle because a twisted molecule can be statistically more planar than one with a planar optimized state. Using this parameter, our group screened currently available high-performance polymer building blocks (Figure 6).[59] After extracting donor and acceptor segments from
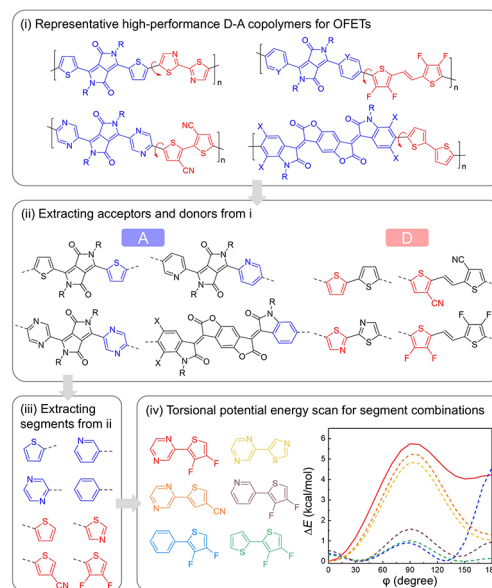

Figure 6. Computer-aided polymer building block screening process: (i) collecting representative high-performance D-A copolymers used for OFETs; (ii) extracting building blocks; (iii) further extracting the segments for simplifying the screening process; and (iv) PES of the dihedral angles of different segment combinations. Reproduced with permission from ref 59. Copyright 2021 The Author(s) under the terms of the Creative Commons CC BY license.

the donor−acceptor (D-A) polymers reported in the literature, relaxed potential energy scans (PESs) were performed at the dihedral angles of adjacent units. We found that the pyrazine (Pz) and 3,4-difluorothiophene (2FT) combination shows the highest rotational barriers with a high $\langle\cos^2\varphi\rangle$ value of 0.9329. The electronegative atom F can form an intramolecular hydrogen bond with the adjacent H atom, and the N atom can form a noncovalent interaction with the S atom, leading to higher rotational barriers. Based on the screening results, we synthesized the polymer P(PzDPP-2FT), which has a single dominant planar backbone, high torsional barrier at each dihedral angle, and zigzag backbone curvature. The polymer is highly dopable and can tolerate dopant-induced disorders. With these features, P(PzDPP-2FT) achieved high n-doped electrical conductivities over 120 S cm^{-1}.

This work inspired us to consider that the backbone planarity in doped states may be important as materials need to operate effectively in heavily doped states for many applications. Subsequently, we designed and synthesized a new DPP-based polymer P(gTDPP2FT) for n-type organic electrochemical transistors (OECTs).[60] Similar to TEs, the whole polymer film in the OECTs is highly doped by electrolytes during operation. At doped states, P(gTDPP2FT) with enhanced doped-state backbone planarity exhibited better negative polaron stability, exhibiting one of the highest n-type OECT performance.

3.3. Side Chain Engineering

Apart from the conjugated backbone, the side chains of polymers could significantly affect the solubility, interchain interactions, and miscibility with dopants. Therefore, side chain engineering also plays an important role in optimizing the thermoelectric performance of conjugated polymers.

Compared with linear alkyl chains, the branched alkyl chains are more favorable for increasing the solubilities of conjugated polymers. Interestingly, a tiny difference in the branching position of chains could bring about a significant difference in the thermoelectric performance of conjugated polymers. Takimiya et al. designed and synthesized two conjugated polymers, PNDTI-BBT-DT and PNDTI-BBT-DP, which have alkyl chains with different branching points.[61] They found that moving the branching points away from the polymer backbones resulted in better crystalline order and mobility in the PNDTI-BBT-DP polymer films. After doping, PNDTI-BBT-DP exhibited 20 times higher electrical conductivity and power factor (14.2 μW m^{-1} K^{-2}). Recently, three thiophene-based TBDOPV copolymers with different branched side chains were reported.[10] The branching points located one, three, and five carbon atoms away from the backbone are named TBDOPV-T-118, TBDOPV-T-318, and TBDOPV-T-518, respectively (Figure 7a). Contrary to expectations, moving the branching positions of alkyl chains farther from the backbone did not significantly decrease the $\pi-\pi$ distance. Instead, it enhanced the intensity of the π-stacking diffraction. To better understand the effect of alkyl side chains, fast scanning calorimetry was used to characterize the melting behaviors of these three polymers. As shown in Figure 7b, TBDOPV-T-518 showed the lowest melting temperature of 16.0 °C, primarily due to its side chains. By splitting the high-temperature peaks, the melting enthalpy can be obtained for polymer films annealed at different temperatures (Figure 7c). Compared with the other two polymers, TBDOPV-T-518 exhibited the weakest temperature dependence of melting enthalpy, suggesting the slowest crystallization rate owing to the weakest thermodynamic driving forces. As a result, TBDOPV-T-518 achieved the highest n-type conductivity of up to 114 S cm^{-1} and the highest power factor of 200 μW m^{-1} K^{-2}.

Besides alkyl chains, polar side chains are also developed because of their ability to enhance the solubility in polar solvents and better miscibility with ionized dopants. For instance, replacing the alkyl side chains in N2200 (also known as P(NDI2OD-T2)) with polar triethylene glycol (TEG) side chains led to the redesigned polymer TEG-N2200.[62] Despite a similar LUMO level, TEG-N2200 exhibited higher doping efficiency and a 200-fold enhancement in electrical conductivity compared to N2200. Coarse-grained molecular dynamics simulations suggested that polar side chains could reduce the dopant clustering and favor the dispersion of the dopant into the host matrix (Figure 7d). Based on this strategy, the authors further developed a copolymer PNDI2C$_8$TEG-2Tz with amphipathic side chain, which contains an alkyl chain segment as a spacer between the polymer backbone and an ethylene glycol type chain segment.[63] The use of this alkyl spacer not only reduces the energetic disorder but also can control the dopant sites away from the backbone, leading to an optimized power factor of 18 μW m^{-1} K^{-2}.

As discussed above, most of these traditional conjugated polymers require long alkyl or ethylene glycol side chains to guarantee good solution processability. However, these solubilizing side chains are insulators, hindering further
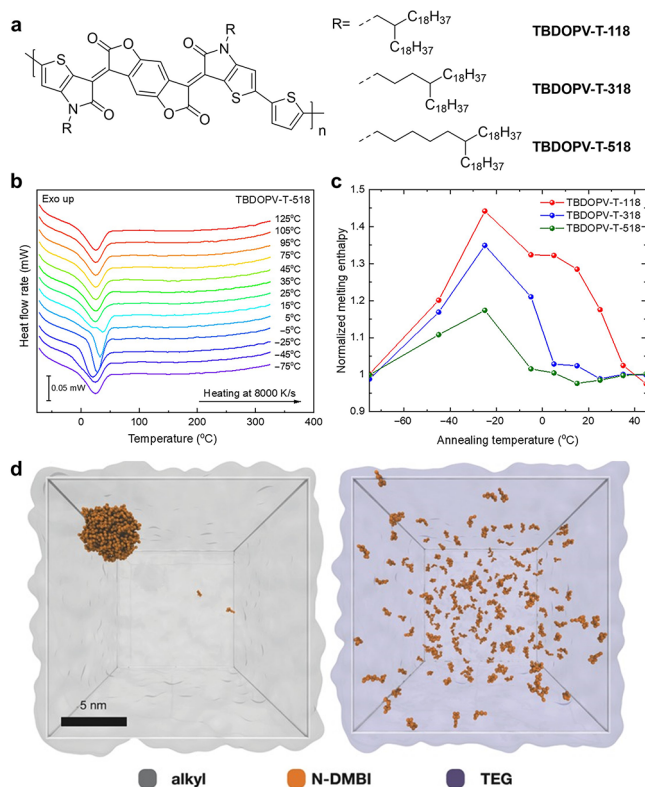

Figure 7. (a) Chemical structure of TBDOPV-T-based polymers with different side chains. (b) Heat flow scans of TBDOPV-T-118, TBDOPV-T-318, and TBDOPV-T-518 films during fast heating with 8000 K s^{-1} after aging at 125 °C for 1 s as the inset scheme of temperature protocols. (c) Melting enthalpy of the split high-temperature peaks for three TBDOPV-T-based polymer films. (d) Representative snapshots of coarse-grained molecular dynamics simulations of *N*-DMBI molecules dissolved in a pure N2200 side chain phase (left) and a pure TEG-N2200 side chain phase (right). (a–c) Reproduced with permission from ref 10. Copyright 2023 The Author(s) under the terms of the Creative Commons CC BY-NC license. (d) Reproduced with permission from ref 62. Copyright 2018 John Wiley and Sons.

enhancement of the thermoelectric performance. As mentioned above, the side chain-free polymer, PBFDO (or n-PBDF), was reported with an impressively high n-type electrical conductivity exceeding 2000 S cm^{-1}.[14,15] However, controlling the doping level in this intrinsically doped polymer remains challenging, leading to a relatively low power factor of 90 μW m^{-1} K^{-2}. Furthermore, the polymer requires high-boiling-point solvents, such as dimethyl sulfoxide (DMSO), for processing, which limits its facile processability. In 2009, Swager et al. reported a cationic polymer, P(PymPh), representing a unique category of n-type conjugated polymers.[64] This cationic polymer is soluble in polar solvents, such as water and 2,2,2-trifluoroethanol. When tested as an n-type TE material, P(PymPh) exhibited a maximum n-type electrical conductivity of 18 S cm^{-1} and a maximum power factor of 0.49 μW m^{-1} K^{-2}.[65]

After this work, cationic polymers have not received enough attention over the years. Recently, our group designed and synthesized a cationic conjugated polymer, P(Py2FT), to further explore the potential of cationic polymers for TEs.[66,67] Compared to traditional polymers with long side chains, P(Py2FT) displayed a significantly reduced lamellar distance and a comparable $\pi-\pi$ stacking distance, promoting more

compact molecular packings for efficient charge transport. After doping, P(Py2FT) exhibited a high n-type electrical conductivity of up to 28.1 S cm^{-1} and a thermoelectric power factor of up to 28.7 μW m^{-1} K^{-2}. These values are already comparable to those of many conventional conjugated polymers. In addition, we demonstrated that cationic building blocks increase the electron density of LUMO across the linkages. This results in a shorter C−C single bond and, consequently, enhanced backbone planarity after doping. Therefore, introducing cationic building blocks is an effective way to enhance the polymer backbone planarity and, thus, charge transport performance after doping.

In this section, we have discussed polymer design strategies from three key perspectives: energy levels, backbone planarity, and side chain engineering. Energy levels and backbone planarity directly impact the doping efficiency and charge carrier mobility. Although side chains do not directly participate in accepting or donating charges and charge transport, they impart their effects through polymer solubility, molecular packing, and dopant miscibility. We believe that further improvements in n-type thermoelectric performance will rely on the design of new polymer building blocks and the utilization of artificial intelligence (AI) optimization techniques. Developing new building blocks with sufficiently low LUMO energy levels appears to be the only feasible way to achieve stable n-type OTE materials. Given the many factors that influence performance, employing AI to consider a broader range of variables may help uncover new structure−property relationships for more effective polymer screening. Additionally, we highlight the potential of side chain-free conjugated polymers, including PBFDO and the cationic conjugated polymers for n-type thermoelectric (TE) materials because of their compact molecular packing with higher proportion of conducting backbone and significantly fewer insulating side chains. However, the lack of side-chain-assisted packing and the repulsive effects introduced by cationic backbones can increase molecular packing disorder, leading to greater energetic disorder and poor interchain charge transport. Therefore, new processing conditions and strategies for tuning molecular packing are needed to further enhance the TE performance of side-chain-free polymers.

4. MOLECULAR DOPING

For doped conjugated polymers, both doping efficiency and energetic disorder play crucial roles. Doping efficiency determines charge carrier concentrations, while energetic disorder largely affects the charge carrier mobilities.[29,68] In this section, we summarize recent strategies to enhance the doping efficiency and reduce doping-induced disorder.

4.1. Doping Efficiency

To improve the doping efficiency, plenty of studies have focused on the molecular design of dopants with low LOMO levels (for p-type) or high HOMO levels (for n-type).[69] Compared to p-type dopants, the design of n-type dopants is more challenging owing to the high-lying HOMO, which makes them unstable under ambient conditions. To solve the dilemma, 1H-benzimidazole-based (DMBI) dopants, such as N-DMBI, have been widely used, which are air-stable precursor molecules and can be converted to active intermediates for n-doping after thermal- or photoactivation.[69,70]

For these dopants, doping takes place through either a hydride transfer from DMBI-H to the host or a hydrogen removal and

electron transfer from DMBI$^{\bullet}$ to the host (Figure 8b).[71,72] Therefore, the single-occupied orbital (SOMO) levels of

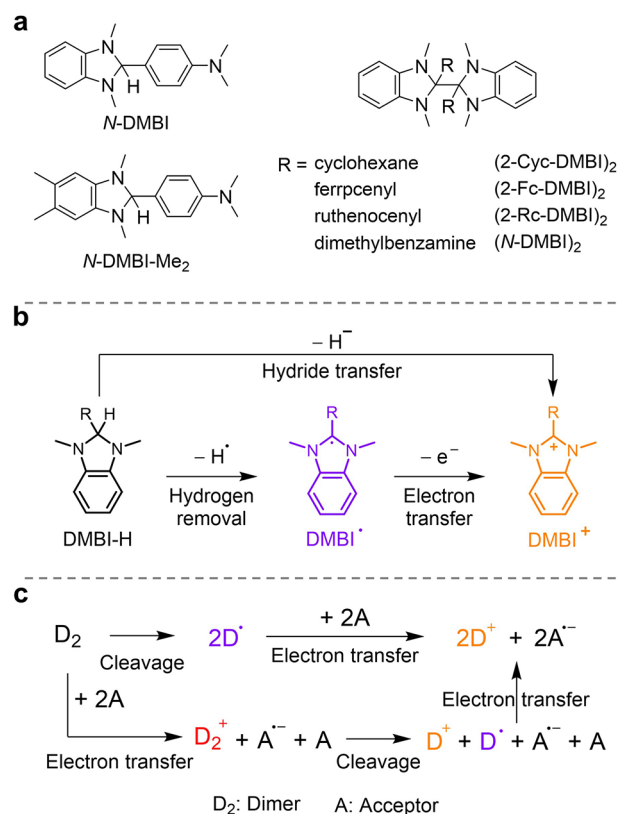**Figure 8.** (a) Chemical structures of some DMBI-based dopants. N-doping pathways of (b) DMBI-H derivatives and (c) DMBI dimers.

DMBI$^{\bullet}$ could be critical for the doping efficiency of DMBI-based dopants. By adding electron-donating methyl and dimethylamine substituents to different positions of the DMBI core, Fabiano, Carlo, and co-workers designed and synthesized a series of benzimidazole-based n-dopants with different SOMO levels.[73] Compared to N-DMBI, N-DMBI-Me$_2$ showed only ~0.3 eV increase in SOMO energy level, whereas it enhanced the electrical conductivity of P(NDI2OD-T2) by more than 1 order of magnitude.

Dimerization is also an effective method to improve the n-doping efficiency and air stability.[74,75] A set of air-stable DMBI dimers, including (N-DMBI)$_2$, (2-Cyc-DMBI)$_2$, (2-Rc-DMBI)$_2$, and (2-Fc-DMBI)$_2$, were synthesized by directly linking two DMBI derivatives at the 2-position (Figure 8a).[76] Compared to previously reported N-DMBI, these DMBI-dimers exhibited stronger doping effect in a more diverse array of materials, which may be ascribed to the particular doping mechanism (Figure 8c): (1) dimer cleavage first, followed by electron transfer from each resulting radical species to the host; (2) electron transfer from the dimer to the host, followed by a bond cleavage, generating one ionic and one radical monomer species, promoting a second electron transfer from radical species.[77]

Hydride and dimer dopants undergo a C−H and C−C bond cleavage reaction, respectively. Thus, the doping efficiency is strongly affected by the thermodynamics and activation energies of the doping reaction. Based on this, Guo, Facchetti, and co-workers reported a general concept of catalyzed n-doping (Figure 9a).[78] Incorporation of a transition metal (e.g., Pt, Au, and Pd) as vapor-deposited nanoparticles or solution-process-
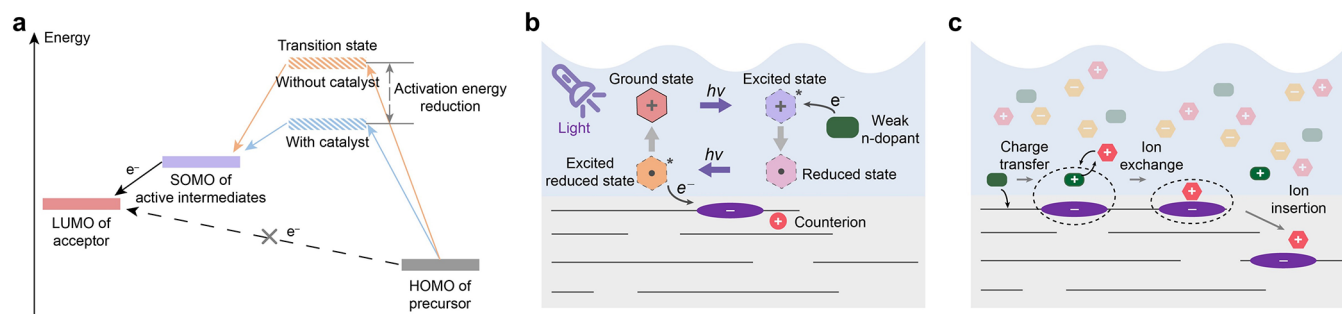
Figure 9. (a) Schematics of the doping process for precursor-type n-dopants with/without transition metal catalysts. (b) Schematic of the photocatalytic n-doping process. (c) Schematic of the ion exchange doping process.

able organometallic complexes (e.g., $Pd_2(dba)_3$) catalyzes the cleavage reaction, enabling greatly increased doping efficiency in a much shorter doping time. Besides transition metals, Kahn et al. demonstrate that photoactivation of the host molecules can also result in kinetically stable and efficient n-doping.[79] Under ultraviolet (UV) irradiation, various host materials with electron affinity down to 2.8 eV can be excited and effectively n-doped by the dimer dopants.

Recently, Fabiano, Yang, and co-workers reported the photocatalytic doping process in quaternary systems comprising a dopant, a photocatalyst (PC), an organic salt, and one of p-type or n-type polymers.[80] Taking n-doping as an example, the charge transfer mechanism of photocatalytic doping is shown in Figure 9b. Neither the dopant nor the PC in the ground state can transfer electrons from or to conjugated polymers. However, when photoexcitation occurs, the excited PC oxidizes the weak n-dopant. Upon photoactivation, the reduced PC at an excited state is capable of reducing n-type polymers. This is a general approach that can be applied to various OSCs and photocatalysts, yielding p-doped, n-doped, and simultaneously p-doped and n-doped OSCs with high conductivity.

The above catalytic doping could accelerate doping reactions but usually could not enhance the doping level when using the same polymer−dopant pair. Thus, methods that can enhance the doping efficiency are desirable. Watanabe, Yamashita, and co-workers reported a general strategy for overcoming the charge-transfer limitations by using ion exchange.[81] The ion exchange doping involves adding a large amount of electrolyte (usually an ionic liquid) to a molecular doping solution. After charge transfer from the dopant to the polymer, the generated dopant radical ions are exchanged with the ions in the electrolyte (Figure 9c). Then, the ions in the electrolyte are incorporated into the polymer film as stable counterions. With an ion exchange efficiency exceeding 99%, this approach substantially increases the doping level. Recently, they found that when 1,3-dimesitylimidazolium cation ($dMesIM^+$) was chosen as the cationic counterion, the n-doped polymer films exhibited high ambient stability.[82] However, thin films doped with other dopants or cations exhibited dedoping upon exposure to humid air. The authors attributed the improved stability of $dMesIM^+$-doped thin films to their face-on-oriented, π-stacked structures. These results indicate that while the ion-exchange doping method kinetically enhances the stability of the doped state, the ultimate stability still depends on the intrinsic stability of the polymer radicals.

Based on this ion exchange method, Watanabe, Yamashita, and co-workers subsequently developed a chemical doping process that is based on proton-coupled electron transfer (PCET) reactions.[83] The polymer films were immersed into

aqueous solutions with benzoquinone (BQ) and hydroquinone (HQ) pairs and hydrophobic molecular ions. The mechanism of doping is assumed to be as follows: in a low-pH aqueous solution, BQ receives two electrons and two protons to transform into the neutral HQ, followed by the insertion of ions into the polymer films to compensate for the injected holes. Unlike the conventional p-type dopants that are deactivated with water in the environment,[84] BQ and HQ do not react with water owing to their weakly oxidizing and reducing nature. In addition, the BQ/HQ PCET reactions and doping level can be precisely and reproducibly tuned by the pH of the doping solution. The estimated ionization potential of the PCET-doped PBTTT was equal to the work function of heavily doped PBTTT, showing the high doping level of this chemical doping method.

4.2. Dopant-Induced Disorder

Introducing dopant counterions increases the charge carrier concentration but at the same time introduces structural and energetic disorder as they often distort molecular conformations and disrupt the molecular packing. Therefore, how a dopant is incorporated into a semiconducting polymer is critical in dictating the resulting charge transport properties. Sirringhaus et al. evaporated the F_4TCNQ dopant on top of a PBTTT layer and allowed the dopant molecule to diffuse into the polymer film.[85] The results show that PBTTT retains its highly ordered lamellar microstructure, where the dopant is preferentially incorporated into the side chain region. With this solid-state diffusion method, they achieve a high electrical conductivity of up to 248 S cm^{-1} in F_4TCNQ-doped PBTTT. Chabinyc and co-workers also demonstrated that for PBTTT, vapor-doping with F_4TCNQ or F_2TCNQ yielded higher electrical conductivity relative to solution-doped films.[86] However, the perturbations to the local polymer structure are minimal and similar for both doping methods, indicating that the enhancement in conductivity here is not related to the local order. On the basis of resonant soft X-ray scattering, vapor-doped samples are shown to have a larger length scale of aligned backbones, resulting in efficient charge transport and thus a higher conductivity relative to solution-doped films. Owing to the better long-range correlation length of backbones, the F_4TCNQ vapor-doped PBTTT yielded a high electrical conductivity of 670 S cm^{-1} and a large power factor of 120 μW m^{-1} K^{-2}.

Apart from doping methods, the choice of dopant counterions also plays an important role in the charge transport properties of semiconducting polymers. The ion exchange doping method discussed above allows for the selection of the dopant counterion systematically from a wide range of counterions. Watanabe et al. demonstrated that the size of the dopant

counterion is critical to the doping efficiency.[81] The salt Li-TFSI composed of small cations (Li$^+$) and large anions (TFSI$^-$), which possess high and low electrostatic surface potentials, respectively, manifests the most efficient anion exchange and doping. The PBTTT films doped with Li-TFSI exhibited the highest electrical conductivity up to 620 S cm^{-1}. However, Sirringhaus et al. discovered that the electrical conductivity of many polymers showed little correlation with the counterion size or shape but exhibited a strong correlation with the paracrystalline disorder (Figure 10b).[87] Their observations
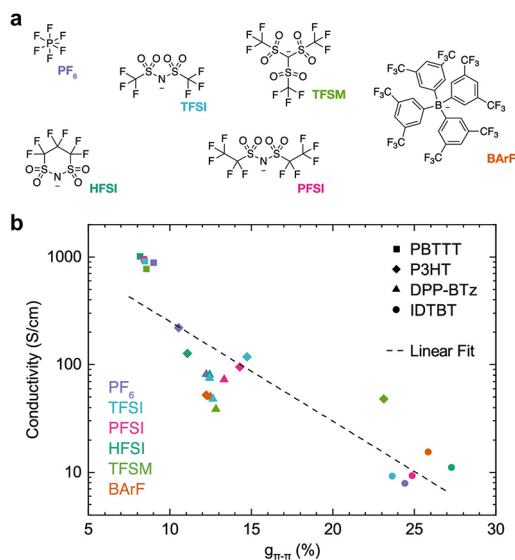

Figure 10. (a) Molecular structures of the anions. (b) Effect of paracrystalline disorder on the conductivity. Conductivity *vs* π-stacking paracrystallinity for four different polymers doped with different ions. Reproduced with permission from ref 87. Copyright 2022, American Chemical Society.

suggest that at high doping levels the most important factor in optimizing the charge transport is the counterion-induced disorder. Recently, they subsequently investigated the charge transport properties of PBTTT as a function of counterion size across a broad range of doping levels.[88] They found that the conductivity is not only weakly dependent on the counterion size at high doping levels, as observed previously, but also extends to surprisingly low doping levels. The absence of a counterion-size effect is explained by heterogeneous doping that involves doping the amorphous domains first before doping the ordered crystalline regions.

These studies underscore the importance of structural disorder in doped semiconducting polymers. Additionally, due to the low dielectric constant of these materials, Coulomb interactions between the charge carriers and counterions are also important. Strong Coulomb interactions could act as Coulomb traps and reduce the number of free carriers.[29,91] To overcome this issue, Schwartz and co-workers designed and synthesized a dodecaborane cluster, DDB-F$_{72}$, which has a high redox potential and steric protection of the core-localized electron density.[92] Unlike F$_4$TCNQ, DDB-F$_{72}$ does not intercalate into the crystalline regions of P3HT. Thus, the counterion resides outside the crystallites, and the unpaired electron on the DDB-F$_{72}$ anion is further separated from the polymer polarons by being confined to the cluster core. As a result, the DDB-F$_{72}$-doped P3HT exhibited electrical conductivities and polaron mobilities roughly an order of magnitude higher than films

doped with F$_4$TCNQ. Based on a similar concept, Koster, Guo, and co-workers reported that thermoelectric properties can be greatly enhanced by overcoming the Coulomb interaction in an n-doped conjugated polymer, PDTzTI.[93] Compared to the reference polymer N2200, PDTzTI chains pack into larger crystal domains, keeping the counterions far from the charges on the polymer chains. Doped PDTzTI exhibits ∼10 times higher free-charge density and 500 times higher conductivity than doped N2200, leading to a power factor of 7.6 μW m^{-1} K^{-2} and ZT of 0.01 at room temperature. These studies use a simplified picture by considering the Coulomb interaction as a distance-dependent function. However, the Coulomb interactions could be significantly influenced by many factors, such as counterion concentrations,[29] the polarization effects of the environment,[94] and the counterion size.[88,95]

Recently, Fediai et al. developed a model to compute the host−dopant interactions V_C for pairs at various distances and relative orientations.[89] This model takes into account three essential factors: distance dependence, the disorder induced by various relative orientations, and the effect of the polarization effects. They showed that the orientation and the quadrupole moments lead to the short-range overscreening effect: at short host−dopant distances, V_C deviates from the classical Coulomb interaction and levels off to a flat electrostatic potential (Figure 11a). In contrast to the intuitive expectation, this effect implies that short host−dopant distances do not necessarily result in a stronger interaction. The charge carriers could move in a flat electrostatic potential rather than be captured into a deep Coulomb trap. Akšamija et al. also considered the role of the screening effect and implemented it in the calculations of
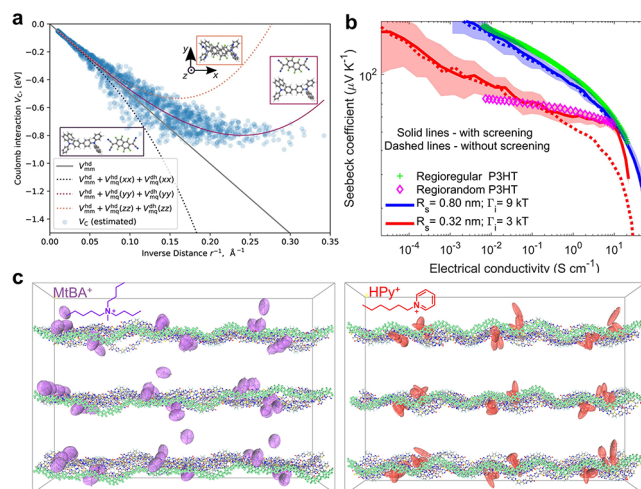

Figure 11. (a) Distance-dependent disorder of V_C. Auxiliary lines are sums of monopole−monopole and monopole−quadrupole interactions in three orthogonal host−dopant orientations, as shown in the insets. (b) Seebeck coefficient against electric conductivity measurements of RR and RRa-P3HT doped with iodine and measured while dedoping. Solid and dashed lines correspond to the case with or without screening, respectively. (c) Molecular dynamic simulation snapshot of the polymer P(PzDPP-2FT) with MtBA$^+$ (left) and HPy$^+$ (right) as the counterions. The polymer backbone in the front is highlighted and the alkyl side chains are hidden for better contrast. (a) Reproduced with permission from ref 89. Copyright 2023 The Author(s) under the terms of the Creative Commons CC BY license. (b) Reproduced with permission from ref 90. Copyright 2023 American Physical Society. (c) Reproduced with permission from ref 11. Copyright 2024 The Author(s) under the terms of the Creative Commons CC BY license.

dopant-induced energetic disorder.[90] Their results showed that screening has a significant impact on the shape of the DOS and consequently on carrier transport, particularly at high doping levels. They proved that when dopants are close to the polymer backbone (small host−dopant distance R_S), the screening effect is stronger, which simultaneously increases the electrical conductivity and Seebeck coefficient (Figure 11b). The thermoelectric power factor is underestimated by a factor of ~10 at high doping concentrations if the screening effect is neglected.

These studies underscored the importance of counterion-induced structural and energetic disorders. Nonetheless, the challenge remains in effectively reducing the counterion-induced disorder in heavily doped semiconducting polymers. Unlike doped inorganic semiconductors, where the dopant atoms are covalently bonded, dopant counterions in polymer films are embedded through intermolecular noncovalent interactions (NCIs), such as electrostatic (ELS) interactions and van der Waals (vdW) forces.[96,97] Our group proposed that these NCIs between the polymer and the dopant counterions are critical for reducing the counterion-induced energetic disorder and reported a general computer-aided counterion screening approach to address this issue.[11] We found that the pronounced vdW interactions between the alkyl counterions and the polymer side chains lead to increased side chain disorder and larger polymer backbone twisting (Figure 11c). In contrast, the stronger ELS interactions stabilize the aromatic counterions around the charged polymer backbone, resulting in enhanced doping efficiency and suppression of the backbone torsions. Using the best aromatic counterion, we achieved a high n-doped electrical conductivity of over 200 S cm^{-1} and an 8-fold increase in the power factor of up to 170 μW m^{-1} K^{-2}.

In this section, we discuss recent advancements aimed at improving doping efficiency and reducing dopant-induced disorder. Efforts have focused on the molecular design of dopants, such as air-stable DMBI-based dopants, and the development of catalytic doping methods, including metal catalysts and photoactivation, to enhance the charge transfer from dopants to polymers. For a specific polymer, there is usually only a very limited number of dopants that can provide efficient doping. The ion exchange doping method successfully expanded this range by allowing the selection of stable counterions from a broader pool. Despite these improvements, challenges remain in reducing structural and energetic disorders induced by dopant counterions at high doping levels, which can disturb polymer packing and hinder charge transport. Selecting appropriate doping methods can help to minimize such disruptions. Recently, attention has turned to the screening of dopant counterions. We propose that carefully designing NCIs between the polymer and dopants could be a key to lowering energetic disorder in heavily doped polymer films. For instance, introducing specific counterion binding sites near the polymer backbone or on the side chains could help to "lock" the counterions and fine-tune the docking position and distribution of counterions, which could lead to further reduced energetic disorder and enhanced TE performance.

5. THERMAL CONDUCTIVITY

Among the three key parameters that determine the ZT value, accurately characterizing thermal conductivity κ usually poses the greatest challenge, especially for polymer thin films. Although the challenge in measurements impedes the understanding of the thermal transport properties of organic

semiconductors, several studies have reported the modification strategies of thermal conductivity. Pipe et al. illustrated that by removing PSS from PEDOT with dimethyl-sulfoxide (DMSO), the cross-plane thermal conductivity of dedoped PEDOT:PSS decreased from 0.30 to 0.22 W m^{-1} K^{-1}, leading to a high ZT value of 0.42 at room temperature.[5] In contrast to the dedoping method, Katz and co-workers reported that the thermal conductivity of a conjugated polymer PDPIN decreases from 0.21 to 0.099 W m^{-1} K^{-1} when the ratio of copolymer ionic dopant PSpF increases from 5 wt % to 75 wt %.[98] It is interesting that the films of 75 wt % PSpF-doped PDPIN present the highest electrical conductivity, power factor, and lowest thermal conductivity, giving a record-high maximum ZT of 0.53 at room temperature for n-type organic TEs.

Recently, Di, Zhao, and co-workers reported a novel polymeric multiheterojunction (PMHJ) design aimed at reducing the thermal conductivity in OTEs. The PMHJ features periodic dual-heterojunction structures, where each period consists of two distinct polymer layers and their interpenetrating interfaces.[99] While the PMHJ shares some geometric similarities with superlattice, the less-ordered polymers and the rough interfaces produce significant interface scattering, even in the in-plane direction. This leads to a marked reduction of the in-plane thermal conductivity: $\kappa_{\parallel}$ can be effectively reduced by the size-effect-enhanced interface scattering, as interface scattering is enhanced by the size effect when the thickness of each polymer layer approaches or is smaller than the phonon-like mean free path along the conjugated backbone and $\pi-\pi$ stacking directions. By creating alternating sub-10 nm PDPPSe-12:PBTTT films with gently interpenetrated interfaces, the PMHJ films showed an impressive low $\kappa_{\parallel}$ of 0.18 W m^{-1} K^{-1} and a maximum ZT of 1.28 at 368 K. This performance not only exceeds that of many commercial inorganic thermoelectric materials but also outperforms current flexible thermoelectric candidates.

Besides conjugated polymers, small molecules, such as fullerene C_{60} and its derivatives, have also been studied as advanced thermoelectric materials owing to their ultralow thermal conductivity (see their chemical structures in Figure 12). Wang et al. found that the thermal conductivity of
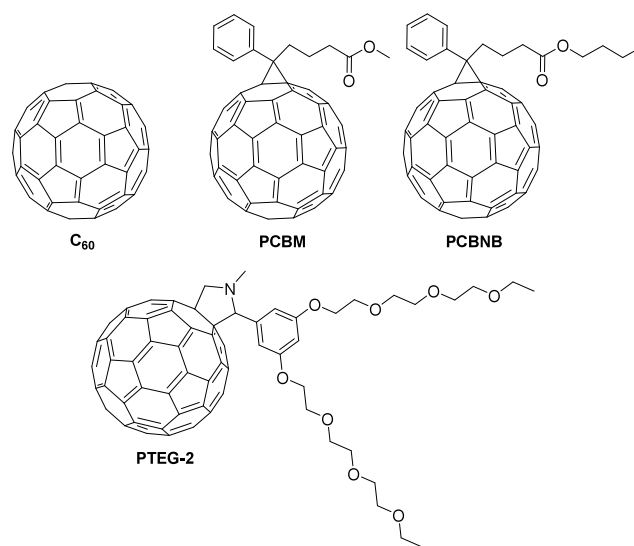

Figure 12. Chemical structures of some small molecules are discussed in this perspective.

disordered C_{60} was only 0.1 W m^{-1} K^{-1} at room temperature. Furthermore, its thermal conductivity can be further reduced by alkyl side chains: phenyl-C61-butyric acid methyl ester (PCBM) and phenyl-C61-butyric acid *n*-buylester (PCBNB) exhibited lower thermal conductivity around 0.05−0.06 W m^{-1} K^{-1}.[100] Using molecular dynamics simulations, Kumar et al. attributed the decrease in thermal conductivity of fullerene derivatives to the significant mismatch of vibrational density of states in the low-frequency regime between buckyball and alkyl chains.[101] Recently, Koster and co-workers explored the thermal conductivity of molecular n-doped fullerene derivatives with different types of side chains.[4] They found that PTEG-2 with "arm-shaped" double-triethylene-glycol-type side chains exhibited not only efficient and thermally stable n-doping but also excellent molecular packing. As a result, the pristine PTEG-2 film displays a very low in-plane thermal conductivity of 0.064 W m^{-1} K^{-1} at room temperature, which slightly increases to 0.086 W m^{-1} K^{-1} after doping with *N*-DMBI.

In this section, we briefly review recent progress in reducing the thermal conductivity in OTEs. While small molecules tend to exhibit significantly lower thermal conductivities, their electrical conductivities are often compromised due to dopant-induced poor molecular packing.[102] The development of PMHJ structures is particularly promising as it highlights that controlling microstructures could be a viable strategy for achieving lower thermal conductivity and improving overall thermoelectric performance in polymer materials. Despite these advancements, understanding thermal transport in OTEs remains a long-standing challenge. Compared to the extensive efforts focused on enhancing electrical conductivity, there has been considerably less research into the structure−property relationships governing thermal conductivity, and effective strategies in this area are still lacking.

6. PROCESSING AND MICROSTRUCTURE CONTROL

In addition to molecular structures and doping strategies, the deposition of conjugated polymers into solid-state thin films from solutions is also critical. Improper control during this process can lead to a high degree of structure and energetic disorders. Therefore, processing optimization is essential for optimizing the microstructures and TE performance of conjugated polymers.

A key advantage of polymer TEs lies in their solution processability to promote large-area and low-temperature processing. To date, various solution processing techniques have been explored such as spin coating, drop casting, solution shearing, and inkjet printing. Spin coating is a popular laboratory-scale deposition technique due to its simplicity and ability to deposit high-quality films across a variety of materials. Bao, Huang, and co-workers developed an "off-center spin" method in which the target substrate is placed away from the central rotation axis.[103] The kinetic nature of the spin-coating process and the rapid solvent evaporation resulted in a highly aligned, metastable crystal packing structure of the small molecule C8-BTBT. Recently, Mei et al. used off-center spin coating at different rates to prepare thin films of n-PBDF with varying thicknesses.[15] Compared to the drop-cast micrometer-thick films, which appeared completely black, the n-PBDF thin films exhibited high transmittance and conductivity, making them suitable for transparent conductors.

Solution shearing often provides conjugated polymer films with higher performance due to its ability to align polymer chains. PEDOT:PSS films deposited by solution shearing have

shown substantially higher electrical conductivity compared to those by spin coating.[104,105] Aligned polymers promote anisotropic structuring within films, leading to a higher conductivity along the deposition direction. Spray-coating is particularly well-suited for large-area processing. Fabiano et al. reported an alcohol-based n-type conductive ink composed of poly(benzimidazobenzophenanthroline) (BBL) doped with poly(ethylenimine) (PEI).[106] The BBL:PEI polymer mixture is prepared via the formulation of an ethanol-based ink, which is processable in air via simple spray-coating. After thermal activation, the n-type BBL:PEI thin films show an electrical conductivity as high as 8 S cm^{-1} with excellent thermal and ambient stability.

The microstructures not only depend on the processing techniques but are also highly sensitive to processing parameters such as solvents, temperature, additives, and concentration. In a polymer solution, the strong interchain interactions can lead to solution-state aggregates, which subsequently affect their solid-state microstructures and optoelectronic properties. Considerable works have unraveled the impacts of such aggregates on the device performance of organic field-effect transistors (OFETs).[107,108] Our group found that controlling the dynamics of polymer aggregates can enhance doping efficiency, leading to improved TE performance.[109] As shown in Figure 13, a good
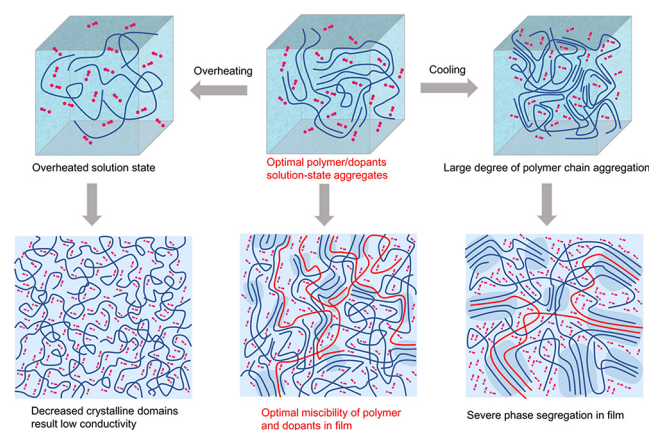

Figure 13. Illustration of the aggregation status of P(PzDPP-CT2) and distribution of *N*-DMBI in solutions and the corresponding film microstructures. Different starting solution-state aggregates can evolve into different solid-state morphologies during device fabrication. Reproduced with permission from ref 109. Copyright 2021 John Wiley and Sons.

solvent and higher temperatures could reduce polymer aggregation and improve miscibility with the dopants. Such solution-state features can be inherited into the polymer solid-state morphologies. However, prolonged cooling can cause phase separation between polymers and dopants due to the reaggregation of the polymers, resulting in low doping efficiency. On the other hand, overheating can disrupt interchain interactions, causing excessive disaggregation of the polymer chains. This results in poor interchain connections, low charge-carrier mobilities, and decreased conductivities. By carefully tuning the polymer aggregates, we were able to adjust the electrical conductivity of the n-type polymer P(PzDPP-CT2) from 2.6 to 32.1 S cm^{-1}. We also demonstrated the broad applicability of our solution-state control strategy in various polymer systems.
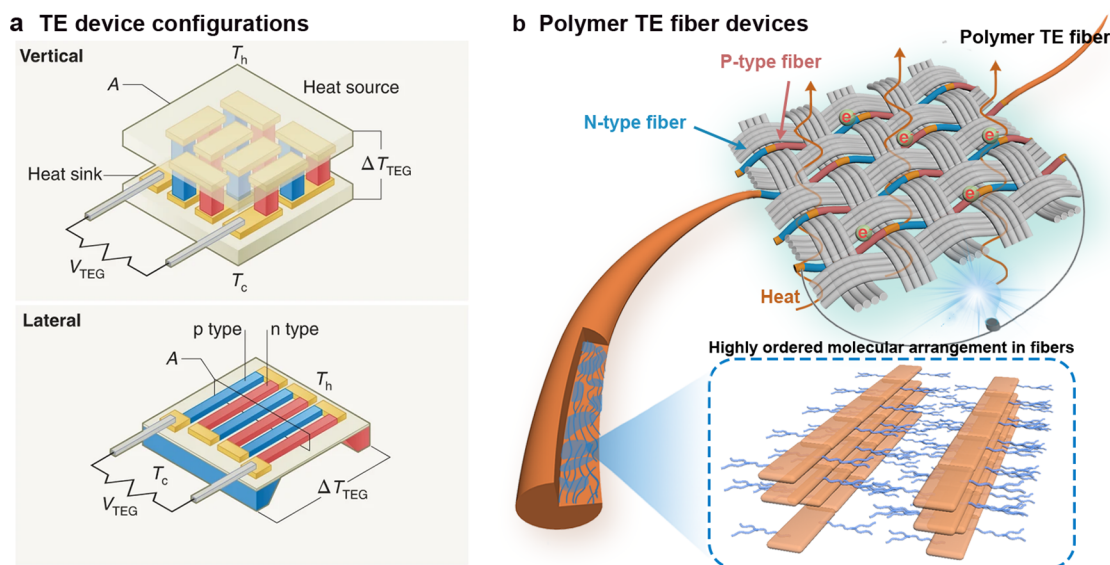
Figure 14. (a) Typical TE device working in vertical and lateral structures. (b) Schematic diagram of polymer TE fibers with highly ordered molecular arrangement and ease of integration into fabrics. (b) Reproduced with permission from ref 119. Copyright 2024 The Author(s) under the terms of the Creative Commons CC BY-NC license.

In this section, we discussed the impact of processing techniques and parameters on the microstructures and TE performances of conjugated polymers. Recent years have witnessed rapid progress in the development of processing methods for the low-cost, high-performance, large-area fabrication of polymer TEs. However, most studies focus on thin-film fabrication, while a complete TE module requires both p- and n-type legs. Thus, thin-film-processing conditions may not apply to thick films or legs often used in TE modules. Another critical issue is the reliance on halogenated solvents, which are environmentally hazardous. As polymer TE technologies advance, green processing techniques, such as using green solvents that reduce environmental impact, should be prioritized. We also highlighted the crucial role that processing parameters play in tuning microstructures. A key challenge is overcoming the trade-off between dopant miscibility and ordered molecular packing, which is essential for high-performance and stable OTEs.

7. POLYMER TES FOR WEARABLE ELECTRONICS

The achievements in polymer TE materials also promote the development of their practical applications. In contrast to inorganic materials, which are mechanically rigid and exhibit the optimum ZT values at high temperatures, polymer TEs have inherent flexibility and show good performance under room temperature. These advantages are desirable for self-powered wearable and smart electronics. However, pristine conjugated polymers usually are still brittle to be used in wearable TEs as dynamic human motions often involve strains of 20−80%.[110] For device flexibility, the deposition of conjugated polymers onto elastomeric soft substrates, including insulating polymers, rubber, paper, and fibers, is the most widely applied strategy.[111] With this method, solution-processable TE materials such as PEDOT and poly[Ni-ett] can be deposited in both the vertical and the horizontal device structure.[112−114] Another popular approach to enhance the mechanical properties of OTEs is blending with stretchable components and dopants.[115,116] To maintain good TE performance of the composites, judiciously chosen processing schemes are necessary. For example, Yang et

al. attempted doping of P3BT:PS blends with F_4TCNQ but observed that the doping process disrupts the formation of P3BT nanowires and results in phase separation.[117] Recently, Crispin and Tybrandt et al. demonstrated an elastomer composite by mixing water-borne polyurethane (WPU) and different ion liquids into PEDOT:PSS solution.[116] The ion liquid acts as a percolation inducer by restructuring the composite films, impeding the agglomeration of WPU particles and plasticizing both the PEDOT and WPU phases. As a result, the optimized films exhibited an electrical conductivity of over 140 S cm^{-1}, a small Young's modulus of less than 7 MPa, and stretchability of over 600%. However, the thermoelectric performances of these stretchable thermoelectric materials remain low along with poor strain recovery capability. Despite the above efforts, most TE devices based on polymers are in thin film states with less or around 100 nm thickness, which are not ideal for integration into a high-efficiency thermoelectric module, since these modules usually require millimeter size blocks or films with tens of micrometers (Figure 14a).[118] Taking into account thermoelectric performance and ease of integration, our group explored the fabrication of stand-alone, strong, tough TE fibers with tens of micrometer size (Figure 14b).[119] As a result, these n-type TE fibers showed a high n-type conductivity of 149 S cm^{-1}, and a power factor of 146 μW m^{-1} K^{-2}, which substantially surpasses that of their film counterparts. The enhancement of the thermoelectric performance is largely due to the improved crystallinity and chain alignment in the fiber. More importantly, fiber-structured devices facilitate seamless integration into fabrics and offer distinctive advantages in wearable TE electronics. These TE fibers were also stretchable with a failure-to-strain of over 50% but showed poor resilience. To date, the realization of truly elastic thermoelectric materials matching the performance of flexible inorganic materials is yet to be achieved and requires further efforts dedicated to polymer TE applications.

8. SUMMARY AND OUTLOOK

Organic thermoelectrics have emerged as a cutting-edge research field and have witnessed fast development in recent

years. In this Perspective, we highlight notable advancements in charge transport mechanism understanding, polymer design, doping strategy, thermal conductivity, morphology control, and applications. Charge transport models provide a theoretical basis for the optimization of the thermoelectric performance, underscoring two important factors: energetic disorder and charge carrier density. Based on these theories, researchers have proposed various polymer design guidelines and doping strategies. These continuous efforts have led to notable progress, with both state-of-the-art p- and n-type polymer TE materials achieving ZT over 0.3 at room temperature range,[5,53] lighting up their potential for practical applications, especially for wearable electronics.

Nonetheless, compared with the well-studied inorganic counterparts that show $ZT > 2$ at high temperatures or $ZT > 0.6$ at room temperature range,[120] the performances of polymer TEs, especially n-type polymers, still lag behind. To break this deadlock, we believe that three key questions need to be addressed. First, polymer TE materials usually need to work under heavily doped states; how can high carrier mobility be maintained after doping? Second, side chains are insulators and do not directly contribute to charge transport; therefore, are they still necessary in polymer TE materials? Third, enlightened by the PMHJ strategy, the thermal conductivity could be further reduced by proper microstructure control. How can this method be used for thick TE films or legs? To these questions, our considerations are as follows: (1) Backbone planarity and rigidity in doped states should be considered. Previous studies have mainly focused on designing planar backbones in neutral states, but large torsional fluctuations may occur in the doped states. Additionally, precisely controlling the distribution of dopant counterions within polymer film could lower the dopant-induced disorder. (2) Side-chain-free polymers may represent the next generation of polymer TE materials. A recent theory study indicated that low-dimensional networks of PBFDO showed electrical behaviors ranging from insulating to semiconducting or metallic, while all three-dimensional (3D) structures consistently exhibited a metallic nature.[44] Thus, designing semiconducting side-chain-free polymers needs to consider their molecular packing and interchain interactions. (3) Nanophase separation is seldom studied in polymer TEs; however, it is widely used in conventional polymer mixtures or block copolymers. Thus, we believe that using some phase separation control strategies in conventional polymers or block copolymers could help to realize PMHJ structures in bulk. In addition, for most n-type polymer TE materials, their stability is still poor and cannot be used under ambient conditions, which is probably the most challenging issue that needs to be addressed before practical applications.

AUTHOR INFORMATION

Corresponding Author

Ting Lei — *Key Laboratory of Polymer Chemistry and Physics of Ministry of Education, School of Materials Science and Engineering, Peking University, Beijing 100871, China;* orcid.org/0000-0001-8190-9483; Email: tinglei@pku.edu.cn

Authors

Xin-Yu Deng — *Key Laboratory of Polymer Chemistry and Physics of Ministry of Education, School of Materials Science and Engineering, Peking University, Beijing 100871, China;* orcid.org/0000-0002-9249-1411

Zhi Zhang — *Key Laboratory of Polymer Chemistry and Physics of Ministry of Education, School of Materials Science and Engineering, Peking University, Beijing 100871, China*

Complete contact information is available at:
https://pubs.acs.org/10.1021/jacsau.4c00638

Author Contributions

The manuscript was written through contributions of all authors. All authors have given approval to the final version of the manuscript. CRediT: **Xin-Yu Deng** validation, writing - original draft, writing - review & editing; **Zhi Zhang** writing - review & editing; **Ting Lei** supervision, writing - review & editing.

Notes

The authors declare no competing financial interest.

ACKNOWLEDGMENTS

REFERENCES

(1) Russ, B.; Glaudell, A.; Urban, J. J.; Chabinyc, M. L.; Segalman, R. A. Organic Thermoelectric Materials for Energy Harvesting and Temperature Control. *Nat. Rev. Mater.* **2016**, *1* (10), 16050.

(2) Zhang, Q.; Sun, Y.; Xu, W.; Zhu, D. Organic Thermoelectric Materials: Emerging Green Energy Materials Converting Heat to Electricity Directly and Efficiently. *Adv. Mater.* **2014**, *26* (40), 6829−6851.

(3) Di, C.-a.; Xu, W.; Zhu, D. Organic Thermoelectrics for Green Energy. *Natl. Sci. Rev.* **2016**, *3* (3), 269−271.

(4) Liu, J.; van der Zee, B.; Alessandri, R.; Sami, S.; Dong, J.; Nugraha, M. I.; Barker, A. J.; Rousseva, S.; Qiu, L.; Qiu, X.; Klasen, N.; Chiechi, R. C.; Baran, D.; Caironi, M.; Anthopoulos, T. D.; Portale, G.; Havenith, R. W. A.; Marrink, S. J.; Hummelen, J. C.; Koster, L. J. A. N-type Organic Thermoelectrics: Demonstration of ZT > 0.3. *Nat. Commun.* **2020**, *11* (1), 5694.

(5) Kim, G. H.; Shao, L.; Zhang, K.; Pipe, K. P. Engineered Doping of Organic Semiconductors for Enhanced Thermoelectric Efficiency. *Nat. Mater.* **2013**, *12* (8), 719−723.

(6) Xu, Y.; Sun, H.; Liu, A.; Zhu, H.-H.; Li, W.; Lin, Y.-F.; Noh, Y.-Y. Doping: A Key Enabler for Organic Transistors. *Adv. Mater.* **2018**, *30* (46), 1801830.

(7) Zhao, W.; Ding, J.; Zou, Y.; Di, C.-a.; Zhu, D. Chemical Doping of Organic Semiconductors for Thermoelectric Applications. *Chem. Soc. Rev.* **2020**, *49* (20), 7210−7228.

(8) Bubnova, O.; Khan, Z. U.; Malti, A.; Braun, S.; Fahlman, M.; Berggren, M.; Crispin, X. Optimization of the Thermoelectric Figure of Merit in the Conducting Polymer Poly(3,4-ethylenedioxythiophene). *Nat. Mater.* **2011**, *10* (6), 429−433.

(9) Lu, Y.; Yu, Z.-D.; Un, H.-I.; Yao, Z.-F.; You, H.-Y.; Jin, W.; Li, L.; Wang, Z.-Y.; Dong, B.-W.; Barlow, S.; Longhi, E.; Di, C.-a.; Zhu, D.; Wang, J.-Y.; Silva, C.; Marder, S. R.; Pei, J. Persistent Conjugated Backbone and Disordered Lamellar Packing Impart Polymers with Efficient n-Doping and High Conductivities. *Adv. Mater.* **2021**, *33* (2), 2005946.

(10) Yu, Z.-D.; Lu, Y.; Wang, Z.-Y.; Un, H.-I.; Zelewski, S. J.; Cui, Y.; You, H.-Y.; Liu, Y.; Xie, K.-F.; Yao, Z.-F.; He, Y.-C.; Wang, J.-Y.; Hu, W.-B.; Sirringhaus, H.; Pei, J. High n-Type and p-Type Conductivities and Power Factors Achieved in a Single Conjugated Polymer. *Sci. Adv.* **2023**, *9* (8), No. eadf3495.

(11) Xiong, M.; Deng, X.-Y.; Tian, S.-Y.; Liu, K.-K.; Fang, Y.-H.; Wang, J.-R.; Wang, Y.; Liu, G.; Chen, J.; Villalva, D. R.; Baran, D.; Gu, X.; Lei, T. Counterion Docking: a General Approach to Reducing

Energetic Disorder in Doped Polymeric Semiconductors. *Nat. Commun.* **2024**, *15* (1), 4972.

(12) Ma, Y.; Zou, Y.; Di, C.-a.; Zhu, D. Introduction of Organic Thermoelectrics. *Organic Thermoelectrics* **2022**, 1−17.

(13) Li, J.-T.; Lei, T. Recent Progress on Addressing the Key Challenges in Organic Thermoelectrics. *Chemistry - An Asian Journal* **2021**, *16* (12), 1508−1518.

(14) Tang, H.; Liang, Y.; Liu, C.; Hu, Z.; Deng, Y.; Guo, H.; Yu, Z.; Song, A.; Zhao, H.; Zhao, D.; Zhang, Y.; Guo, X.; Pei, J.; Ma, Y.; Cao, Y.; Huang, F. A Solution-Processed n-Type Conducting Polymer with Ultrahigh Conductivity. *Nature* **2022**, *611* (7935), 271−277.

(15) Ke, Z.; Abtahi, A.; Hwang, J.; Chen, K.; Chaudhary, J.; Song, I.; Perera, K.; You, L.; Baustert, K. N.; Graham, K. R.; Mei, J. Highly Conductive and Solution-Processable n-Doped Transparent Organic Conductor. *J. Am. Chem. Soc.* **2023**, *145* (6), 3706−3715.

(16) Mott, N. The Mobility Edge Since 1967. *J. Phys. C: Solid State Phys.* **1987**, *20* (21), 3075.

(17) Salleo, A.; Chen, T. W.; Völkel, A. R.; Wu, Y.; Liu, P.; Ong, B. S.; Street, R. A. Intrinsic Hole Mobility and Trapping in a Regioregular Poly(thiophene). *Phys. Rev. B* **2004**, *70* (11), 115311.

(18) Chang, J.-F.; Sirringhaus, H.; Giles, M.; Heeney, M.; McCulloch, I. Relative Importance of Polaron Activation and Disorder on Charge Transport in High-Mobility Conjugated Polymer Field-Effect Transistors. *Phys. Rev. B* **2007**, *76* (20), 205204.

(19) Thorpe, M. F.; Weaire, D. Electronic Density of States of Amorphous Si and Ge. *Phys. Rev. Lett.* **1971**, *27* (23), 1581−1584.

(20) Vissenberg, M. C. J. M.; Matters, M. Theory of the Field-Effect Mobility in Amorphous Organic Transistors. *Phys. Rev. B* **1998**, *57* (20), 12964−12967.

(21) Mott, N. F.; Davis, E. A.; Weiser, K. Electronic Processes in Non-Crystalline Materials. *Phys. Today* **1972**, *25* (12), 55−55.

(22) Abdalla, H.; Zuo, G.; Kemerink, M. Range and Energetics of Charge Hopping in Organic Semiconductors. *Phys. Rev. B* **2017**, *96* (24), 241202.

(23) Nardes, A. M.; Kemerink, M.; Janssen, R. A. J. Anisotropic Hopping Conduction in Spin-Coated PEDOT:PSS Thin Films. *Phys. Rev. B* **2007**, *76* (8), 085208.

(24) Kang, S. D.; Snyder, G. J. Charge-Transport Model for Conducting Polymers. *Nat. Mater.* **2017**, *16* (2), 252−257.

(25) Abutaha, A.; Kumar, P.; Yildirim, E.; Shi, W.; Yang, S.-W.; Wu, G.; Hippalgaonkar, K. Correlating Charge and Thermoelectric Transport to Paracrystallinity in Conducting Polymers. *Nat. Commun.* **2020**, *11* (1), 1737.

(26) Statz, M.; Venkateshvaran, D.; Jiao, X.; Schott, S.; McNeill, C. R.; Emin, D.; Sirringhaus, H.; Di Pietro, R. On the Manifestation of Electron-Electron Interactions in the Thermoelectric Response of Semicrystalline Conjugated Polymers with Low Energetic Disorder. *Commun. Phys.* **2018**, *1* (1), 16.

(27) Thomas, E. M.; Popere, B. C.; Fang, H.; Chabinyc, M. L.; Segalman, R. A. Role of Disorder Induced by Doping on the Thermoelectric Properties of Semiconducting Polymers. *Chem. Mater.* **2018**, *30* (9), 2965−2972.

(28) Boyle, C. J.; Upadhyaya, M.; Wang, P.; Renna, L. A.; Lu-Diaz, M.; Pyo Jeong, S.; Hight-Huf, N.; Korugic-Karasz, L.; Barnes, M. D.; Aksamija, Z.; Venkataraman, D. Tuning Charge Transport Dynamics via Clustering of Doping in Organic Semiconductor Thin Films. *Nat. Commun.* **2019**, *10* (1), 2827.

(29) Arkhipov, V. I.; Emelianova, E. V.; Heremans, P.; Bässler, H. Analytic Model of Carrier Mobility in Doped Disordered Organic Semiconductors. *Phys. Rev. B* **2005**, *72* (23), 235202.

(30) Arkhipov, V. I.; Heremans, P.; Emelianova, E. V.; Bässler, H. Effect of Doping on the Density-of-States Distribution and Carrier Hopping in Disordered Organic Semiconductors. *Phys. Rev. B* **2005**, *71* (4), 045214.

(31) Gregory, S. A.; Hanus, R.; Atassi, A.; Rinehart, J. M.; Wooding, J. P.; Menon, A. K.; Losego, M. D.; Snyder, G. J.; Yee, S. K. Quantifying Charge Carrier Localization in Chemically Doped Semiconducting Polymers. *Nat. Mater.* **2021**, *20*, 1414.

(32) Xuan, Y.; Liu, X.; Desbief, S.; Leclère, P.; Fahlman, M.; Lazzaroni, R.; Berggren, M.; Cornil, J.; Emin, D.; Crispin, X. Thermoelectric Properties of Conducting Polymers: The Case of Poly(3-hexylthiophene). *Phys. Rev. B* **2010**, *82* (11), 115454.

(33) Tanaka, H.; Kanahashi, K.; Takekoshi, N.; Mada, H.; Ito, H.; Shimoi, Y.; Ohta, H.; Takenobu, T. Thermoelectric Properties of a Semicrystalline Polymer Doped beyond the Insulator-to-Metal Transition by Electrolyte Gating. *Sci. Adv.* **2020**, *6* (7), No. eaay8065.

(34) Kaiser, A. B. Thermoelectric Power and Conductivity of Heterogeneous Conducting Polymers. *Phys. Rev. B* **1989**, *40* (5), 2806−2813.

(35) Jones, T. E.; Ogden, T. R.; McGinnis, W. C.; Butler, W. F.; Gottfredson, D. M. Electronic Properties of Polyacetylene Doped with FeCl₃. *J. Chem. Phys.* **1985**, *83* (5), 2532−2537.

(36) Chiang, C. K.; Fincher, C. R.; Park, Y. W.; Heeger, A. J.; Shirakawa, H.; Louis, E. J.; Gau, S. C.; MacDiarmid, A. G. Electrical Conductivity in Doped Polyacetylene. *Phys. Rev. Lett.* **1977**, *39* (17), 1098−1101.

(37) Chiang, C. K.; Park, Y. W.; Heeger, A. J.; Shirakawa, H.; Louis, E. J.; MacDiarmid, A. G. Conducting Polymers: Halogen Doped Polyacetylene. *J. Chem. Phys.* **1978**, *69* (11), 5098−5104.

(38) Park, Y. W.; Heeger, A. J.; Druy, M. A.; MacDiarmid, A. G. Electrical Transport in Doped Polyacetylene. *J. Chem. Phys.* **1980**, *73* (2), 946−957.

(39) Blackburn, J. L.; Kang, S. D.; Roos, M. J.; Norton-Baker, B.; Miller, E. M.; Ferguson, A. J. Intrinsic and Extrinsically Limited Thermoelectric Transport within Semiconducting Single-Walled Carbon Nanotube Networks. *Adv. Electron. Mater.* **2019**, *5* (11), 1800910.

(40) Shi, K.; Zhang, F.; Di, C.-A.; Yan, T.-W.; Zou, Y.; Zhou, X.; Zhu, D.; Wang, J.-Y.; Pei, J. Toward High Performance n-Type Thermoelectric Materials by Rational Modification of BDPPV Backbones. *J. Am. Chem. Soc.* **2015**, *137* (22), 6979−6982.

(41) Yan, X.; Xiong, M.; Li, J.-T.; Zhang, S.; Ahmad, Z.; Lu, Y.; Wang, Z.-Y.; Yao, Z.-F.; Wang, J.-Y.; Gu, X.; Lei, T. Pyrazine-Flanked Diketopyrrolopyrrole (DPP): a New Polymer Building Block for High-Performance n-Type Organic Thermoelectrics. *J. Am. Chem. Soc.* **2019**, *141* (51), 20215−20221.

(42) Feng, K.; Guo, H.; Wang, J.; Shi, Y.; Wu, Z.; Su, M.; Zhang, X.; Son, J. H.; Woo, H. Y.; Guo, X. Cyano-Functionalized Bithiophene Imide-Based n-Type Polymer Semiconductors: Synthesis, Structure-Property Correlations, and Thermoelectric Performance. *J. Am. Chem. Soc.* **2021**, *143* (3), 1539−1552.

(43) Tang, H.; Cai, H.; Zhao, H.; Liu, Z.; Tan, R.; Huang, F. A Solution-Processed n-Type Conducting Polymer Without Side Chains Formed via Nonmetal-Participated Polymerization and in Situ n-Doping. *CCS Chem.* **2023**, *5* (11), 2534−2544.

(44) Ni, X.; Li, H.; Coropceanu, V.; Brédas, J.-L. Dimensionality-Dependent Electronic Properties of the Highly Conducting n-Type Polymer, Poly(benzodifurandione). *ACS Mater. Lett.* **2024**, *6*, 2569−2576.

(45) Wu, W.; Liu, Y.; Zhu, D. π-Conjugated Molecules with Fused rings for Organic Field-Effect Transistors: Design, Synthesis and Applications. *Chem. Soc. Rev.* **2010**, *39* (5), 1489−1502.

(46) Ding, L.; Yu, Z.-D.; Wang, X.-Y.; Yao, Z.-F.; Lu, Y.; Yang, C.-Y.; Wang, J.-Y.; Pei, J. Polymer Semiconductors: Synthesis, Processing, and Applications. *Chem. Rev.* **2023**, *123* (12), 7421−7497.

(47) Huang, H.; Yang, L.; Facchetti, A.; Marks, T. J. Organic and Polymeric Semiconductors Enhanced by Noncovalent Conformational Locks. *Chem. Rev.* **2017**, *117* (15), 10291−10318.

(48) Huang, H.; Chen, Z.; Ortiz, R. P.; Newman, C.; Usta, H.; Lou, S.; Youn, J.; Noh, Y.-Y.; Baeg, K.-J.; Chen, L. X.; Facchetti, A.; Marks, T. Combining Electron-Neutral Building Blocks with Intramolecular "Conformational Locks" Affords Stable, High-Mobility p- and n-Channel Polymer Semiconductors. *J. Am. Chem. Soc.* **2012**, *134* (26), 10966−10973.

(49) Lei, T.; Xia, X.; Wang, J.-Y.; Liu, C.-J.; Pei, J. Conformation Locked" Strong Electron-Deficient Poly(p-Phenylene Vinylene) Derivatives for Ambient-Stable N-Type Field-Effect Transistors:

Synthesis, Properties, and Effects of Fluorine Substitution Position. *J. Am. Chem. Soc.* **2014**, *136* (5), 2135−2141.

(50) Zheng, Y.-Q.; Lei, T.; Dou, J.-H.; Xia, X.; Wang, J.-Y.; Liu, C.-J.; Pei, J. Strong Electron-Deficient Polymers Lead to High Electron Mobility in Air and Their Morphology-Dependent Transport Behaviors. *Adv. Mater.* **2016**, *28* (33), 7213−7219.

(51) Jackson, N. E.; Savoie, B. M.; Kohlstedt, K. L.; Olvera de la Cruz, M.; Schatz, G. C.; Chen, L. X.; Ratner, M. A. Controlling Conformations of Conjugated Polymers and Small Molecules: the Role of Nonbonding Interactions. *J. Am. Chem. Soc.* **2013**, *135* (28), 10475−10483.

(52) Wang, S.; Sun, H.; Erdmann, T.; Wang, G.; Fazzi, D.; Lappan, U.; Puttisong, Y.; Chen, Z.; Berggren, M.; Crispin, X.; Kiriy, A.; Voit, B.; Marks, T. J.; Fabiano, S.; Facchetti, A. A Chemically Doped Naphthalenediimide-Bithiazole Polymer for n-Type Organic Thermoelectrics. *Adv. Mater.* **2018**, *30* (31), 1801898.

(53) Yang, C.-Y.; Jin, W.-L.; Wang, J.; Ding, Y.-F.; Nong, S.; Shi, K.; Lu, Y.; Dai, Y.-Z.; Zhuang, F.-D.; Lei, T.; Di, C.-A.; Zhu, D.; Wang, J.-Y.; Pei, J. Enhancing the n-Type Conductivity and Thermoelectric Performance of Donor-Acceptor Copolymers through Donor Engineering. *Adv. Mater.* **2018**, *30* (43), 1802850.

(54) Lu, Y.; Yu, Z.-D.; Zhang, R.-Z.; Yao, Z.-F.; You, H.-Y.; Jiang, L.; Un, H.-I.; Dong, B.-W.; Xiong, M.; Wang, J.-Y.; Pei, J. Rigid Coplanar Polymers for Stable n-Type Polymer Thermoelectrics. *Angew. Chem., Int. Ed.* **2019**, *58* (33), 11390−11394.

(55) Onwubiko, A.; Yue, W.; Jellett, C.; Xiao, M.; Chen, H.-Y.; Ravva, M. K.; Hanifi, D. A.; Knall, A.-C.; Purushothaman, B.; Nikolka, M.; Flores, J.-C.; Salleo, A.; Bredas, J.-L.; Sirringhaus, H.; Hayoz, P.; McCulloch, I. Fused Electron Deficient Semiconducting Polymers for Air Stable Electron Transport. *Nat. Commun.* **2018**, *9* (1), 416.

(56) Chen, H.; Moser, M.; Wang, S.; Jellett, C.; Thorley, K.; Harrison, G. T.; Jiao, X.; Xiao, M.; Purushothaman, B.; Alsufyani, M.; Bristow, H.; De Wolf, S.; Gasparini, N.; Wadsworth, A.; McNeill, C. R.; Sirringhaus, H.; Fabiano, S.; McCulloch, I. Acene Ring Size Optimization in Fused Lactam Polymers Enabling High n-Type Organic Thermoelectric Performance. *J. Am. Chem. Soc.* **2021**, *143* (1), 260−268.

(57) Xiao, M.; Carey, R. L.; Chen, H.; Jiao, X.; Lemaur, V.; Schott, S.; Nikolka, M.; Jellett, C.; Sadhanala, A.; Rogers, S.; Senanayak, S. P.; Onwubiko, A.; Han, S.; Zhang, Z.; Abdi-Jalebi, M.; Zhang, Y.; Thomas, T. H.; Mahmoudi, N.; Lai, L.; Selezneva, E.; Ren, X.; Nguyen, M.; Wang, Q.; Jacobs, I.; Yue, W.; McNeill, C. R.; Liu, G.; Beljonne, D.; McCulloch, I.; Sirringhaus, H. Charge Transport Physics of a Unique Class of Rigid-Rod Conjugated Polymers with Fused-Ring Conjugated Units Linked by Double Carbon-Carbon Bonds. *Sci. Adv.* **2021**, *7* (18), No. eabe5280.

(58) Che, Y.; Perepichka, D. F. Quantifying Planarity in the Design of Organic Electronic Materials. *Angew. Chem., Int. Ed.* **2021**, *60* (3), 1364−1373.

(59) Yan, X.; Xiong, M.; Deng, X.-Y.; Liu, K.-K.; Li, J.-T.; Wang, X.-Q.; Zhang, S.; Prine, N.; Zhang, Z.; Huang, W.; Wang, Y.; Wang, J.-Y.; Gu, X.; So, S. K.; Zhu, J.; Lei, T. Approaching Disorder-Tolerant Semiconducting Polymers. *Nat. Commun.* **2021**, *12* (1), 5723.

(60) Li, P.; Shi, J.; Lei, Y.; Huang, Z.; Lei, T. Switching P-Type to High-Performance n-Type Organic Electrochemical Transistors via Doped State Engineering. *Nat. Commun.* **2022**, *13* (1), 5970.

(61) Wang, Y.; Nakano, M.; Michinobu, T.; Kiyota, Y.; Mori, T.; Takimiya, K. Naphthodithiophenediimide-Benzobisthiadiazole-Based Polymers: Versatile n-Type Materials for Field-Effect Transistors and Thermoelectric Devices. *Macromolecules* **2017**, *50* (3), 857−864.

(62) Liu, J.; Qiu, L.; Alessandri, R.; Qiu, X.; Portale, G.; Dong, J.; Talsma, W.; Ye, G.; Sengrian, A. A.; Souza, P. C. T.; Loi, M. A.; Chiechi, R. C.; Marrink, S. J.; Hummelen, J. C.; Koster, L. J. A. Enhancing Molecular n-Type Doping of Donor-Acceptor Copolymers by Tailoring Side Chains. *Adv. Mater.* **2018**, *30* (7), 1704630.

(63) Liu, J.; Ye, G.; Potgieser, H. G. O.; Koopmans, M.; Sami, S.; Nugraha, M. I.; Villalva, D. R.; Sun, H.; Dong, J.; Yang, X.; Qiu, X.; Yao, C.; Portale, G.; Fabiano, S.; Anthopoulos, T. D.; Baran, D.; Havenith, R. W. A.; Chiechi, R. C.; Koster, L. J. A. Amphipathic Side Chain of a

Conjugated Polymer Optimizes Dopant Location toward Efficient n-Type Organic Thermoelectrics. *Adv. Mater.* **2021**, *33* (4), 2006694.

(64) Izuhara, D.; Swager, T. M. Poly(Pyridinium Phenylene)s: Water-Soluble n-Type Polymers. *J. Am. Chem. Soc.* **2009**, *131* (49), 17724−17725.

(65) Hwang, S.; Potscavage, W. J.; Yang, Y. S.; Park, I. S.; Matsushima, T.; Adachi, C. Solution-Processed Organic Thermoelectric Materials Exhibiting Doping-Concentration-Dependent Polarity. *Phys. Chem. Chem. Phys.* **2016**, *18* (42), 29199−29207.

(66) Li, J.-L.; Deng, X.-Y.; Chen, J.; Fu, P.-X.; Tian, S.-Y.; Wang, Y.; Gu, X.; Lei, T. Cationic Conjugated Polymers with Enhanced Doped-State Planarity for n-Type Organic Thermoelectrics. *CCS Chem.* **2024**, *0* (0), 1−10.

(67) Li, P.; Sun, W.; Li, J.; Chen, J.-P.; Wang, X.; Mei, Z.; Jin, G.; Lei, Y.; Xin, R.; Yang, M.; Xu, J.; Pan, X.; Song, C.; Deng, X.-Y.; Lei, X.; Liu, K.; Wang, X.; Zheng, Y.; Zhu, J.; Lv, S.; Zhang, Z.; Dai, X.; Lei, T. N-type semiconducting hydrogel. *Science* **2024**, *384* (6695), 557−563.

(68) Pasveer, W. F.; Cottaar, J.; Tanase, C.; Coehoorn, R.; Bobbert, P. A.; Blom, P. W. M.; de Leeuw, D. M.; Michels, M. A. J. Unified Description of Charge-Carrier Mobilities in Disordered Semiconducting Polymers. *Phys. Rev. Lett.* **2005**, *94* (20), 206601.

(69) Scaccabarozzi, A. D.; Basu, A.; Aniés, F.; Liu, J.; Zapata-Arteaga, O.; Warren, R.; Firdaus, Y.; Nugraha, M. I.; Lin, Y.; Campoy-Quiles, M.; Koch, N.; Müller, C.; Tsetseris, L.; Heeney, M.; Anthopoulos, T. D. Doping Approaches for Organic Semiconductors. *Chem. Rev.* **2022**, *122* (4), 4420−4492.

(70) Wei, P.; Oh, J. H.; Dong, G.; Bao, Z. Use of a 1H-Benzoimidazole Derivative as an n-Type Dopant and To Enable Air-Stable Solution-Processed n-Channel Organic Thin-Film Transistors. *J. Am. Chem. Soc.* **2010**, *132* (26), 8852−8853.

(71) Zeng, Y.; Zheng, W.; Guo, Y.; Han, G.; Yi, Y. Doping Mechanisms of N-DMBI-H for Organic Thermoelectrics: Hydrogen Removal vs. Hydride Transfer. *J. Mater. Chem. A* **2020**, *8* (17), 8323−8328.

(72) Naab, B. D.; Guo, S.; Olthof, S.; Evans, E. G. B.; Wei, P.; Millhauser, G. L.; Kahn, A.; Barlow, S.; Marder, S. R.; Bao, Z. Mechanistic Study on the Solution-Phase n-Doping of 1,3-Dimethyl-2-aryl-2,3-dihydro-1H-benzoimidazole Derivatives. *J. Am. Chem. Soc.* **2013**, *135* (40), 15018−15025.

(73) Riera-Galindo, S.; Orbelli Biroli, A.; Forni, A.; Puttisong, Y.; Tessore, F.; Pizzotti, M.; Pavlopoulou, E.; Solano, E.; Wang, S.; Wang, G.; Ruoko, T.-P.; Chen, W. M.; Kemerink, M.; Berggren, M.; di Carlo, G.; Fabiano, S. Impact of Singly Occupied Molecular Orbital Energy on the n-Doping Efficiency of Benzimidazole Derivatives. *ACS Appl. Mater. Interfaces* **2019**, *11* (41), 37981−37990.

(74) Un, H.-I.; Gregory, S. A.; Mohapatra, S. K.; Xiong, M.; Longhi, E.; Lu, Y.; Rigin, S.; Jhulki, S.; Yang, C.-Y.; Timofeeva, T. V.; Wang, J.-Y.; Yee, S. K.; Barlow, S.; Marder, S. R.; Pei, J. Understanding the Effects of Molecular Dopant on n-Type Organic Thermoelectric Properties. *Adv. Energy Mater.* **2019**, *9* (24), 1900817.

(75) Perry, E. E.; Chiu, C.-Y.; Moudgil, K.; Schlitz, R. A.; Takacs, C. J.; O'Hara, K. A.; Labram, J. G.; Glaudell, A. M.; Sherman, J. B.; Barlow, S.; Hawker, C. J.; Marder, S. R.; Chabinyc, M. L. High Conductivity in a Nonplanar n-Doped Ambipolar Semiconducting Polymer. *Chem. Mater.* **2017**, *29* (22), 9742−9750.

(76) Naab, B. D.; Zhang, S.; Vandewal, K.; Salleo, A.; Barlow, S.; Marder, S. R.; Bao, Z. Effective Solution- and Vacuum-Processed n-Doping by Dimers of Benzimidazoline Radicals. *Adv. Mater.* **2014**, *26* (25), 4268−4272.

(77) Zhang, S.; Naab, B. D.; Jucov, E. V.; Parkin, S.; Evans, E. G. B.; Millhauser, G. L.; Timofeeva, T. V.; Risko, C.; Brédas, J.-L.; Bao, Z.; Barlow, S.; Marder, S. R. N-Dopants Based on Dimers of Benzimidazoline Radicals: Structures and Mechanism of Redox Reactions. *Chem.—Eur. J.* **2015**, *21* (30), 10878−10885.

(78) Guo, H.; Yang, C.-Y.; Zhang, X.; Motta, A.; Feng, K.; Xia, Y.; Shi, Y.; Wu, Z.; Yang, K.; Chen, J.; Liao, Q.; Tang, Y.; Sun, H.; Woo, H. Y.; Fabiano, S.; Facchetti, A.; Guo, X. Transition Metal-Catalysed Molecular n-Doping of Organic Semiconductors. *Nature* **2021**, *599* (7883), 67−73.

(79) Lin, X.; Wegner, B.; Lee, K. M.; Fusella, M. A.; Zhang, F.; Moudgil, K.; Rand, B. P.; Barlow, S.; Marder, S. R.; Koch, N.; Kahn, A. Beating the Thermodynamic Limit with Photo-Activation of n-Doping in Organic Semiconductors. *Nat. Mater.* **2017**, *16* (12), 1209−1215.

(80) Jin, W.; Yang, C.-Y.; Pau, R.; Wang, Q.; Tekelenburg, E. K.; Wu, H.-Y.; Wu, Z.; Jeong, S. Y.; Pitzalis, F.; Liu, T.; He, Q.; Li, Q.; Huang, J.-D.; Kroon, R.; Heeney, M.; Woo, H. Y.; Mura, A.; Motta, A.; Facchetti, A.; Fahlman, M.; Loi, M. A.; Fabiano, S. Photocatalytic Doping of Organic Semiconductors. *Nature* **2024**, *630* (8015), 96−101.

(81) Yamashita, Y.; Tsurumi, J.; Ohno, M.; Fujimoto, R.; Kumagai, S.; Kurosawa, T.; Okamoto, T.; Takeya, J.; Watanabe, S. Efficient Molecular Doping of Polymeric Semiconductors Driven by Anion Exchange. *Nature* **2019**, *572* (7771), 634−638.

(82) Yamashita, Y.; Kohno, S.; Longhi, E.; Jhulki, S.; Kumagai, S.; Barlow, S.; Marder, S. R.; Takeya, J.; Watanabe, S. N-type Molecular Doping of a Semicrystalline Conjugated Polymer Through Cation Exchange. *Commun. Mater.* **2024**, *5* (1), 79.

(83) Ishii, M.; Yamashita, Y.; Watanabe, S.; Ariga, K.; Takeya, J. Doping of Molecular Semiconductors Through Proton-Coupled Electron Transfer. *Nature* **2023**, *622* (7982), 285−291.

(84) Jacobs, I. E.; Moulé, A. J. Controlling Molecular Doping in Organic Semiconductors. *Adv. Mater.* **2017**, *29* (42), 1703063.

(85) Kang, K.; Watanabe, S.; Broch, K.; Sepe, A.; Brown, A.; Nasrallah, I.; Nikolka, M.; Fei, Z.; Heeney, M.; Matsumoto, D.; Marumoto, K.; Tanaka, H.; Kuroda, S.-i.; Sirringhaus, H. 2D Coherent Charge Transport in Highly Ordered Conducting Polymers Doped by Solid State Diffusion. *Nat. Mater.* **2016**, *15* (8), 896−902.

(86) Patel, S. N.; Glaudell, A. M.; Peterson, K. A.; Thomas, E. M.; O'Hara, K. A.; Lim, E.; Chabinyc, M. L. Morphology Controls the Thermoelectric Power Factor of a Doped Semiconducting Polymer. *Sci. Adv.* **2017**, *3* (6), No. e1700434.

(87) Jacobs, I. E.; D'Avino, G.; Lemaur, V.; Lin, Y.; Huang, Y.; Chen, C.; Harrelson, T. F.; Wood, W.; Spalek, L. J.; Mustafa, T.; O'Keefe, C. A.; Ren, X.; Simatos, D.; Tjhe, D.; Statz, M.; Strzalka, J. W.; Lee, J.-K.; McCulloch, I.; Fratini, S.; Beljonne, D.; Sirringhaus, H. Structural and Dynamic Disorder, not Ionic Trapping, Controls Charge Transport in Highly Doped Conducting Polymers. *J. Am. Chem. Soc.* **2022**, *144* (7), 3005−3019.

(88) Chen, C.; Jacobs, I. E.; Kang, K.; Lin, Y.; Jellett, C.; Kang, B.; Lee, S. B.; Huang, Y.; BaloochQarai, M.; Ghosh, R.; Statz, M.; Wood, W.; Ren, X.; Tjhe, D.; Sun, Y.; She, X.; Hu, Y.; Jiang, L.; Spano, F. C.; McCulloch, I.; Sirringhaus, H. Observation of Weak Counterion Size Dependence of Thermoelectric Transport in Ion Exchange Doped Conducting Polymers Across a Wide Range of Conductivities. *Adv. Energy Mater.* **2023**, *13* (9), 2202797.

(89) Armleder, J.; Neumann, T.; Symalla, F.; Strunk, T.; Olivares Peña, J. E.; Wenzel, W.; Fediai, A. Controlling Doping Efficiency in Organic Semiconductors by Tuning Short-Range Overscreening. *Nat. Commun.* **2023**, *14* (1), 1356.

(90) Duhandžić, M.; Lu-Dìaz, M.; Samanta, S.; Venkataraman, D.; Akšamija, Z. Carrier Screening Dontrols Transport in Conjugated Polymers at High Doping Concentrations. *Phys. Rev. Lett.* **2023**, *131* (24), 248101.

(91) Tietze, M. L.; Benduhn, J.; Pahner, P.; Nell, B.; Schwarze, M.; Kleemann, H.; Krammer, M.; Zojer, K.; Vandewal, K.; Leo, K. Elementary Steps in Electrical Doping of Organic Semiconductors. *Nat. Commun.* **2018**, *9* (1), 1182.

(92) Aubry, T. J.; Axtell, J. C.; Basile, V. M.; Winchell, K. J.; Lindemuth, J. R.; Porter, T. M.; Liu, J.-Y.; Alexandrova, A. N.; Kubiak, C. P.; Tolbert, S. H.; Spokoyny, A. M.; Schwartz, B. J. Dodecaborane-Based Dopants Designed to Shield Anion Electrostatics Lead to Increased Carrier Mobility in a Doped Conjugated Polymer. *Adv. Mater.* **2019**, *31* (11), 1805647.

(93) Liu, J.; Shi, Y.; Dong, J.; Nugraha, M. I.; Qiu, X.; Su, M.; Chiechi, R. C.; Baran, D.; Portale, G.; Guo, X.; Koster, L. J. A. Overcoming Coulomb Interaction Improves Free-Charge Generation and Thermo-electric Properties for n-Doped Conjugated Polymers. *ACS Energy Lett.* **2019**, *4* (7), 1556−1564.

(94) Schwarze, M.; Gaul, C.; Scholz, R.; Bussolotti, F.; Hofacker, A.; Schellhammer, K. S.; Nell, B.; Naab, B. D.; Bao, Z.; Spoltore, D.; Vandewal, K.; Widmer, J.; Kera, S.; Ueno, N.; Ortmann, F.; Leo, K. Molecular Parameters Responsible for Thermally Activated Transport in Doped Organic Semiconductors. *Nat. Mater.* **2019**, *18* (3), 242−248.

(95) Jacobs, I. E.; Lin, Y.; Huang, Y.; Ren, X.; Simatos, D.; Chen, C.; Tjhe, D.; Statz, M.; Lai, L.; Finn, P. A.; Neal, W. G.; D'Avino, G.; Lemaur, V.; Fratini, S.; Beljonne, D.; Strzalka, J.; Nielsen, C. B.; Barlow, S.; Marder, S. R.; McCulloch, I.; Sirringhaus, H. High-Efficiency Ion-Exchange Doping of Conducting Polymers. *Adv. Mater.* **2022**, *34* (22), 2102988.

(96) Lüssem, B.; Keum, C.-M.; Kasemann, D.; Naab, B.; Bao, Z.; Leo, K. Doped Organic Transistors. *Chem. Rev.* **2016**, *116* (22), 13714−13751.

(97) Dou, J.-H.; Yu, Z.-A.; Zhang, J.; Zheng, Y.-Q.; Yao, Z.-F.; Tu, Z.; Wang, X.; Huang, S.; Liu, C.; Sun, J.; Yi, Y.; Cao, X.; Gao, Y.; Wang, J.-Y.; Pei, J. Organic Semiconducting Alloys with Tunable Energy Levels. *J. Am. Chem. Soc.* **2019**, *141* (16), 6561−6568.

(98) Han, J.; Jiang, Y.; Tiernan, E.; Ganley, C.; Song, Y.; Lee, T.; Chiu, A.; McGuiggan, P.; Adams, N.; Clancy, P.; Russell, T. P.; Hopkins, P. E.; Thon, S. M.; Tovar, J. D.; Katz, H. E. Blended Conjugated Host and Unconjugated Dopant Polymers Towards n-type All-Polymer Con-ductors and High-ZT Thermoelectrics. *Angew. Chem., Int. Ed.* **2023**, *62* (23), No. e202219313.

(99) Wang, D.; Ding, J.; Ma, Y.; Xu, C.; Li, Z.; Zhang, X.; Zhao, Y.; Zhao, Y.; Di, Y.; Liu, L.; Dai, X.; Zou, Y.; Kim, B.; Zhang, F.; Liu, Z.; McCulloch, I.; Lee, M.; Chang, C.; Yang, X.; Wang, D.; Zhang, D.; Zhao, L.-D.; Di, C.-a.; Zhu, D. Multi-Heterojunctioned Plastics with High Thermoelectric Figure of Merit. *Nature* **2024**, *632* (8025), 528−535.

(100) Wang, X.; Liman, C. D.; Treat, N. D.; Chabinyc, M. L.; Cahill, D. G. Ultralow Thermal Conductivity of Fullerene Derivatives. *Phys. Rev. B* **2013**, *88* (7), 075310.

(101) Chen, L.; Wang, X.; Kumar, S. Thermal Transport in Fullerene Derivatives Using Molecular Dynamics Simulations. *Sci. Rep.* **2015**, *5* (1), 12763.

(102) Ge, G.-Y.; Li, J.-T.; Wang, J.-R.; Xiong, M.; Dong, X.; Li, Z.-J.; Li, J.-L.; Cao, X.-Y.; Lei, T.; Wang, J.-L. Unveiling the Interplay among End Group, Molecular Packing, Doping Level, and Charge Transport in n-Doped Small-Molecule Organic Semiconductors. *Adv. Funct. Mater.* **2022**, *32* (7), 2108289.

(103) Yuan, Y.; Giri, G.; Ayzner, A. L.; Zoombelt, A. P.; Mannsfeld, S. C. B.; Chen, J.; Nordlund, D.; Toney, M. F.; Huang, J.; Bao, Z. Ultra-High Mobility Transparent Organic Thin Film Transistors Grown by an Off-Centre Spin-Coating Method. *Nat. Commun.* **2014**, *5* (1), 3005.

(104) Hinckley, A. C.; Andrews, S. C.; Dunham, M. T.; Sood, A.; Barako, M. T.; Schneider, S.; Toney, M. F.; Goodson, K. E.; Bao, Z. Achieving High Thermoelectric Performance and Metallic Transport in Solvent-Sheared PEDOT:PSS. *Adv. Electron. Mater.* **2021**, *7* (3), 2001190.

(105) Worfolk, B. J.; Andrews, S. C.; Park, S.; Reinspach, J.; Liu, N.; Toney, M. F.; Mannsfeld, S. C. B.; Bao, Z. Ultrahigh Electrical Conductivity in Solution-Sheared Polymeric Transparent Films. *Proc. Natl. Acad. Sci. U. S. A.* **2015**, *112* (46), 14138−14143.

(106) Yang, C.-Y.; Stoeckel, M.-A.; Ruoko, T.-P.; Wu, H.-Y.; Liu, X.; Kolhe, N. B.; Wu, Z.; Puttisong, Y.; Musumeci, C.; Massetti, M.; Sun, H.; Xu, K.; Tu, D.; Chen, W. M.; Woo, H. Y.; Fahlman, M.; Jenekhe, S. A.; Berggren, M.; Fabiano, S. A High-Conductivity n-Type Polymeric Ink for Printed Electronics. *Nat. Commun.* **2021**, *12* (1), 2354.

(107) Xu, Z.; Park, K. S.; Kwok, J. J.; Lin, O.; Patel, B. B.; Kafle, P.; Davies, D. W.; Chen, Q.; Diao, Y. Not All Aggregates Are Made the Same: Distinct Structures of Solution Aggregates Drastically Modulate Assembly Pathways, Morphology, and Electronic Properties of Conjugated Polymers. *Adv. Mater.* **2022**, *34* (32), 2203055.

(108) Zheng, Y.-Q.; Yao, Z.-F.; Lei, T.; Dou, J.-H.; Yang, C.-Y.; Zou, L.; Meng, X.; Ma, W.; Wang, J.-Y.; Pei, J. Unraveling the Solution-State Supramolecular Structures of Donor-Acceptor Polymers and their Influence on Solid-State Morphology and Charge-Transport Proper-ties. *Adv. Mater.* **2017**, *29* (42), 1701072.

(109) Xiong, M.; Yan, X.; Li, J.-T.; Zhang, S.; Cao, Z.; Prine, N.; Lu, Y.; Wang, J.-Y.; Gu, X.; Lei, T. Efficient n-Doping of Polymeric Semiconductors through Controlling the Dynamics of Solution-State Polymer Aggregates. *Angew. Chem., Int. Ed.* **2021**, *60* (15), 8189−8197.

(110) Someya, T.; Bao, Z.; Malliaras, G. G. The Rise of Plastic Bioelectronics. *Nature* **2016**, *540* (7633), 379−385.

(111) Ma, Y.; Di, C.-a.; Zhu, D. Advances in Organic Thermoelectric Devices for Multiple Applications. *Adv. phys. res* **2023**, *2* (11), 2300027.

(112) Sheng, P.; Sun, Y.; Jiao, F.; Di, C.; Xu, W.; Zhu, D. A Novel Cuprous Ethylenetetrathiolate Coordination Polymer: Structure Characterization, Thermoelectric Property Optimization and a Bulk Thermogenerator Demonstration. *Synth. Met.* **2014**, *193*, 1−7.

(113) Sun, Y.; Sheng, P.; Di, C.; Jiao, F.; Xu, W.; Qiu, D.; Zhu, D. Organic Thermoelectric Materials and Devices Based on p- and n-Type Poly(metal 1,1,2,2-ethenetetrathiolate)s. *Adv. Mater.* **2012**, *24* (7), 932−937.

(114) Du, Y.; Cai, K.; Chen, S.; Wang, H.; Shen, S. Z.; Donelson, R.; Lin, T. Thermoelectric Fabrics: Toward Power Generating Clothing. *Sci. Rep.* **2015**, *5* (1), 6411.

(115) Kiefer, D.; Yu, L.; Fransson, E.; Gómez, A.; Primetzhofer, D.; Amassian, A.; Campoy-Quiles, M.; Müller, C. A Solution-Doped Polymer Semiconductor:Insulator Blend for Thermoelectrics. *Adv. Sci.* **2017**, *4* (1), 1600203.

(116) Kim, N.; Lienemann, S.; Petsagkourakis, I.; Alemu Mengistie, D.; Kee, S.; Ederth, T.; Gueskine, V.; Leclère, P.; Lazzaroni, R.; Crispin, X.; Tybrandt, K. Elastic conducting polymer composites in thermoelectric modules. *Nat. Commun.* **2020**, *11* (1), 1424.

(117) Lu, G.; Bu, L.; Li, S.; Yang, X. Bulk Interpenetration Network of Thermoelectric Polymer in Insulating Supporting Matrix. *Adv. Mater.* **2014**, *26* (15), 2359−2364.

(118) Zhang, Q.; Deng, K.; Wilkens, L.; Reith, H.; Nielsch, K. Micro-Thermoelectric Devices. *Nat. Electron.* **2022**, *5* (6), 333−347.

(119) Zhang, Z.; Li, P.; Xiong, M.; Zhang, L.; Chen, J.; Lei, X.; Pan, X.; Wang, X.; Deng, X.-Y.; Shen, W.; Mei, Z.; Liu, K.-K.; Liu, G.; Huang, Z.; Lv, S.; Shao, Y.; Lei, T. Continuous Production of Ultratough Semiconducting Polymer Fibers with High Electronic Performance. *Sci. Adv.* **2024**, *10* (14), No. eadk0647.

(120) Yan, Q.; Kanatzidis, M. G. High-Performance Thermoelectrics and Challenges for Practical Devices. *Nat. Mater.* **2022**, *21* (5), 503−513.